

# ESTIMATION OF EDDY-CURRENT LOSSES BY MEANS OF VARIATIONAL METHODS

J. Puczyński, W. Popow, R. Sikora, M. Gromz  
Polytechnic of Szczecin, Poland.

## ABSTRACT

The paper deals with a method for estimation of eddy-current losses in thin conducting sheets having various shapes. It is assumed that the magnetic field due to eddy-currents is negligible compared with the exciting flux. The Ritz and Trefftz variational methods are applied to give an upper and a lower bound for the exact value of power losses. The method is demonstrated by examples.

## 1. INTRODUCTION

In the electromagnetic field analysis by means of variational methods the problem of accuracy assumes some importance, since there is no general method allowing to determine the exactness of the solution obtained.

However, if the parameters proportional to the energy are to be determined (e.g. capacitance, inductance resistance) an upper and a lower bound for the correct value can be calculated applying dual functionals minimization. This method have been used for the estimation of capacitance<sup>3</sup> and inductance<sup>4</sup>.

In this paper Ritz and Trefftz variational methods are applied to the calculation of power losses due to eddy-currents induced in thin sheets. It is assumed that the secondary magnetic field produced by eddy-currents is negligible comparing the exciting

flux (for the detailed discussion of the validity of this assumption see the Reference<sup>3</sup>). In this case the current flow function  $I$  defined in References<sup>5,10,11,12,14</sup> can be introduced and the problem can be described by the Poisson equation<sup>12</sup>

$$\Delta I = \omega B d \gamma \quad (1)$$

accompanied by the boundary condition

$$I|_r = 0 \quad (1a)$$

where  $\omega$  denotes an angular frequency,  $B$  is the exciting magnetic flux density,  $d$  and  $\gamma$  are thickness and conductivity of the sheet, and  $r$  denotes the boundary of investigated region.

## 2. THEORY

The Dirichlet boundary problem (1a) for the Poisson equation (1) is equivalent to the problem of minimization of the functional

$$F_R = \iint_D (\text{grad}^2 I + 2\omega B d \gamma I) dD \quad (2)$$

in the Ritz method<sup>6,7,9</sup>, or

$$F_T = \iint_D \text{grad}^2 I dD \quad (3)$$

in the Trefftz method<sup>1,2,8,13</sup>.

The functional (3) reaches its minimum for the correct value  $I_c$  being the solution of the Dirichlet problem (1a) for eqn. (1).

$$F_c = \iint_D \text{grad}^2 I_c dD \quad (4)$$

(subscript  $c$  denotes the correct value).

For any other trial function  $I$  we have:

$$F_T \gg F_C \quad (5)$$

Taking into account Green's formula

$$\iint_D \text{grad}^2 I_C dD + \iint_D I_C \Delta I_C dD = \oint_{\Gamma} I_C \frac{\partial I_C}{\partial n} dD \quad (6)$$

the functional (2) can be written in the following form

$$F_{RC} = - \iint_D \text{grad}^2 I_C dD \quad (7)$$

Formulas (6) and (7) yield

$$F_{RC} = - F_C \quad (8)$$

It is obvious that

$$F_R \gg F_{RC} \quad (9)$$

and from the eqn. (8)

$$F_C \gg -F_R \quad (10)$$

Inequalities (5) and (10) give the base for the determination of an upper and a lower bound for the correct value of the functional

$$-F_R \leq F_C \leq F_T \quad (11)$$

It is a very close relation between the functional value and the power losses due to eddy-currents.

The power losses can be calculated by the formula:

$$P = \frac{d}{\gamma} \iint_D |\dot{I}|^2 dx dy \quad (12)$$

which after substituting for  $|\dot{I}|^2$  takes the form<sup>12</sup>

$$P = \frac{4}{\gamma d} \iint_D \text{grad}^2 I dD = \frac{F_C}{\gamma d} \quad (13)$$

From the eqns (11) and (13) it results

$$P_R \leq P_C \leq P_T \quad (14)$$

where  $P_R, P_T$  denote power losses calculated by means of Ritz and Trefftz method respectively and  $P_C$  is an exact value of power losses.

### 3. EXAMPLES

#### 3.1. Rectangular plate.

Let us consider a thin rectangular conducting plate placed in the uniform magnetic field. The plate is shown in the Fig. 1.

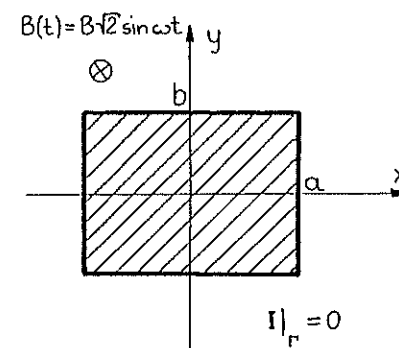


Fig. 1. Rectangular plate under investigation.

The power losses in the plate are calculated by means of the Ritz, Kantorovich, Trefftz and modified Trefftz method. In the papers<sup>10, 12</sup> the Ritz and Kantorovich method have been applied to the problem

losses calculation in a rectangular plate. Both Ritz and Kantorovich method gives a lower bound of the power value. From the Ritz method, applying the second approximate, we obtain

$$P_R = 0.07025 \frac{ab}{a^2+b^2} \alpha \quad (15)$$

where  $\alpha = (4ab\omega B)^2 d\gamma$

and from the Kantorovich method

$$P_K = \frac{b\alpha}{12a} \left( 1 - \frac{2}{\sqrt{10}} \frac{b}{a} \tanh \frac{\sqrt{10}}{2} \frac{a}{b} \right) \quad (16)$$

In order to determine an upper bound of the power value the Trefftz method and modified Trefftz method are used.

The trial current flow function  $I$  has been chosen in the form

$$I = \omega B d\gamma \left[ -\frac{1}{4}(x^2+y^2) + C_1(x^2-y^2) + C_2(x^4-6x^2y^2+y^4) \right] \quad (17)$$

After minimization of the functional (3) we obtain the following formula for the power losses

$$P_T = \frac{\alpha}{ab} \left[ \frac{1}{3}(a^2+b^2) \left( \frac{1}{16} - C_1^2 \right) - \frac{1}{6} C_1(a^2-b^2) + \frac{4}{5} C_1 C_2(a^4-b^4) - \frac{1}{15} C_2(3a^2-b^2)(a^2-3b^2) + \frac{4}{35} C_2^2(a^2+b^2)(5a^4+2a^2b^2+5b^4) \right] \quad (18)$$

where

$$C_1 = \frac{(a^2-b^2)(a^4+20a^2b^2+b^4)}{4(a^2-b^2)(a^4+13a^2b^2+b^4)},$$

$$C_2 = -\frac{35a^2b^2}{24(a^2+b^2)(a^4+a^2b^2+b^4)}$$

To improve the accuracy the modified Trefftz method is applied<sup>15</sup>. This method is somewhat similar to the Kantorovich method.

The trial function is chosen in the form

$$I = \omega B d\gamma \left( -\frac{1}{2}x^2 + C_1 \cosh \frac{k}{a} y \cos \frac{k}{a} x \right) \quad (19)$$

which satisfies the Poisson equation (1) and includes indefinite coefficients  $C_1$  and  $k$ .

Applying the 'classical' Trefftz minimization method we evaluate the coefficient  $C_1$  and we have the functional minimum value as the function of the parameter  $k$ :

$$F_{min} = f(k) \quad (20)$$

Minimizing the function  $F_{min}$  with respect to the parameter  $k$ , according to the formula

$$\frac{\partial F_{min}}{\partial k} = 0 \quad (21)$$

we obtain

$$P_{TH} = \frac{a\alpha}{12b} \left[ 1 - \frac{12a^2}{k^2b^2} \sinh^2 \left( \frac{kb}{a} \right) \cdot \frac{(k \cos k - \sin k)^2}{\frac{a}{b} \sinh \left( \frac{2kb}{a} \right) - \sin 2k} \right] \quad (22)$$

In the Fig. 2 the function  $k=f(a/b)$  is plotted.

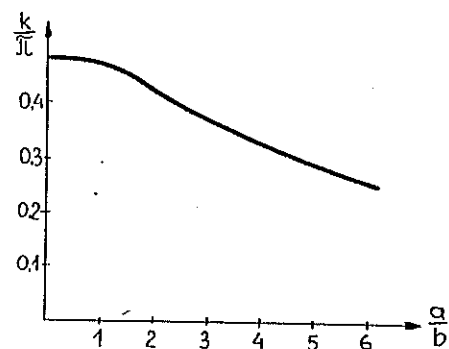


Fig. 2. The  $k$ -parameter versus dimensions of rectangle ratio.

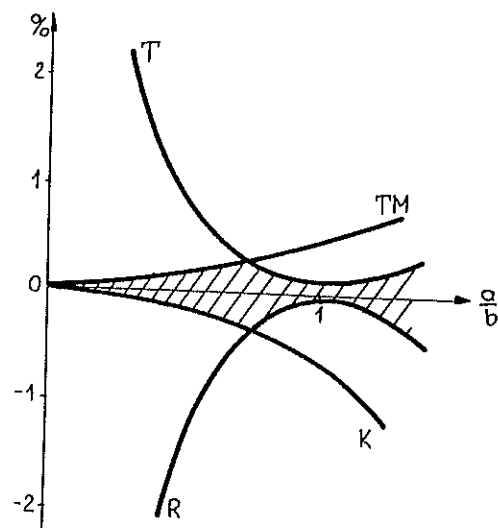


Fig. 3. The error of calculation versus  $a/b$  ratio for:

- R - Ritz method
- T - Trefftz method
- K - Kantorovich method
- TN - modified Trefftz method.

For the rectangular plate the correct value of power losses can be calculated by means of the separation of variables method<sup>10</sup> and the error of the calculations by means of the methods mentioned above can be determined. In the Fig. 3 the error is plotted against the  $a/b$  ratio.

The shadowed region shows the area in which the maximum of the error value is contained. Usually the average of the  $P_R$  and  $P_T$  value or  $P_K$  and  $P_{TN}$  value is taken as the solution.

### 3.2. Sector of the circle.

As the second example we consider a plate of the shape of a sector of the circle illustrated in the Fig. 4.

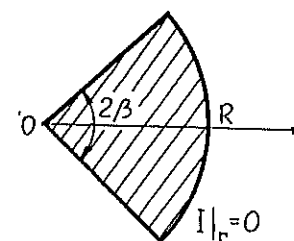


Fig. 4. The sector of the circle.

The power losses are calculated by means of the Ritz, Kantorovich, Trefftz and modified Trefftz method. The results are as follows:

- from the Ritz method, applying the trial function

$$I = \alpha_1 r(r-R)(\varphi^2 - \beta^2) \quad (23)$$

we have

$$P_R = \frac{\omega^2 B^2 d \gamma R^4 \beta^3}{18(1+0.8\beta^2)} \quad (24)$$

- from the Kantorovich method

$$P_K = \frac{1}{12} \omega^2 B^2 d \gamma R^4 \beta \left(1 - \frac{16\sqrt{2}\beta}{\sqrt{2}\beta}\right) \quad (25)$$

- from the Trefftz method, using the approximate

$$I = \omega d \gamma B \left( \frac{1}{4} r^2 + \alpha_1 r \cos \varphi \right) \quad (26)$$

we obtain

$$P_T = \frac{1}{8} \omega^2 B^2 d \gamma R^4 \beta \left[ 1 - \frac{8}{9} \frac{\sin^2 \beta}{\beta^2} \right] \quad (27)$$

and

- from the modified Trefftz method, applying the approximation of current flow function I in the form

$$I = \omega d \gamma B \left( \frac{1}{4} r^2 + \alpha_1 r^p \cos p \varphi \right) \quad (28)$$

we have

$$P_{TM} = \omega^2 B^2 d \gamma R^4 \left[ \frac{1}{8} \beta - \frac{\sin^2 \beta}{(p+2)^2 p \beta} \right] \quad (29)$$

where  $p$  can be determined from the relation

$$\frac{19 p \beta}{p \beta} = \frac{2(p+2)}{3p+2} \quad (30)$$

The results obtained are shown in the Fig. 5 as the functions of the angle  $\beta$ . The exact value of the power losses is contained in the shadowed region.

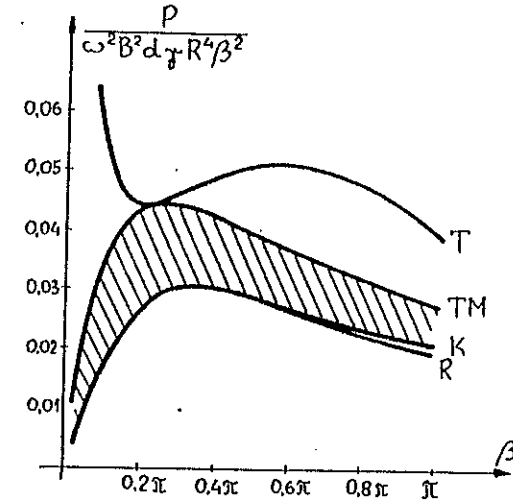


Fig. 5. Power losses in the sector of the circle as the function of the angle  $\beta$  calculated by means of:

- R - Ritz method
- T - Trefftz method
- K - Kantorovich method
- TM - modified Trefftz method.

#### 4. CONCLUSIONS

In the paper a method for estimation of the power losses in thin conducting plates is introduced. Application of both Ritz and Trefftz or Kantorovich and modified Trefftz method gives an upper and a lower bound for the power value. The approximate value of the power losses can be calculated as the average of  $P_R$  and  $P_T$  or  $P_K$  and  $P_{TM}$  values. It has been shown that using simultaneously these four methods the error can be estimated and minimized.

## 5. REFERENCES

1. Birman, M. Variational Methods for Solution of the Boundary Problems Similar to the Trefftz Method. Vestnik Leningrad University, № 13, 1956 (in Russian).
2. Collatz, L. Numerische Behandlung von Differentialgleichungen, Springer-Verlag, 1955, Berlin-Göttingen-Heidelberg.
3. Gramz, M. Purczyński, J. Sikora, R. Calculation of Eddy-Currents Induced in Thin Curved Sheets. to be published in Proc. of COMPUMAG, Grenoble, 1978.
4. Hammond, P. Physical Basic of the Variational Method for the Computation of Magnetic Field Problems. Proc. of COMPUMAG, Oxford, 1976.
5. De Mey, G. A Method for Calculating Eddy Currents in Plates of Arbitrary Geometry. Archiv. f. Elektrotechn., 56 (1974), 137-140.
6. Nikulin, S. G. Variational Methods in Mathematical Physics. Moskva, 1970 (in Russian).
7. Purczyński, J. Slot Leakage Field Analysis by Means of the Variational Methods. Archiv. f. Elektr. (to be published).
8. Purczyński, J. Capacity Estimation by Means of Ritz and Trefftz Methods. Archiv. f. Elektrot., 59 (1977), 269-274.
9. Purczyński, J. Rolicz, P. Sikora, R. Use of Ritz and Bubnov-Galerkin Methods for Calculation of Inductance and Impedance of Conductors. Archiv. f. Elektrot., 57 (1975).
10. Purczyński, J. Sikora, R. Lipiński, W. Eddy Currents in Sheets. Archivum Elektrot., 24 (1972) 727-741. (in Polish).
11. Schieber, D. Unipolar Induction Braking of Thin Metal Sheet. Proc. IEE, 119 (1972), 1499.
12. Sikora, R. Purczyński, J. Lipiński, W. Gramz, M. Use of Variational Methods to the Eddy-Currents Calculation in Thin Conducting Plates. to be published in the IEEE Trans. on Magnetics, Sept. 1978.
13. Trefftz, E. Ein Gegenstück zum Ritschen Verfahren Verhandl. d.2. Intern. Kongress. f. Technische Mechanik, Zürich, 1926.
14. Zlatev, MP. Etude des champs electriques non potentiels. RGE, 1956, nr 9.
15. Purczyński, J. Popow, W. Anwendung der Methode der Zweifachen Minimierung zur bestimmung der Wirbelstromleistungsverluste. to be published in Z.IET.

TWODIMENSIONAL FINITE ELEMENT ANALYSIS  
OF LOW FREQUENCY ELECTROMAGNETIC FIELDS IN LINEAR MEDIA

P. Janeček  
ASEA-KDT, S-72183 Västerås, Sweden

ABSTRACT

An application is presented of the F.E.M. to the solution of the equation for the vector potential (the "diffusion" equation) in two space dimensions. The resulting computer program ECSTASY (Eddy Current & Skin effect Twodimensional Analysis System) using complex arithmetics can handle problems where material properties are time- and field-independent but can vary in space. The boundary conditions can be of Dirichlet or Neumann type. Applied voltages or total currents can be specified for groups of conductors in parallel. The mesh is triangular, the approximating polynomials of up to the 5th degree. An example of the computer-generated field plot for an actual application is presented.

1. INTRODUCTION

Eddy currents occur in all types of electrical equipment subjected to a time-varying magnetic field. They can be put to good use as in induction furnaces, or, as is often the case, one wishes to reduce the loss of effect caused by them. In order to equip the designing engineer with a computational tool which would enable him to calculate the magnetic field resulting from his design, a computer program has been developed at the Department for System Analysis and Technical Programming (KDT) of the ASEA Co, Västerås, Sweden.

The program uses the finite element technique to solve the equation for the vector potential for cases of special symmetry, i.e. with translational or rotational invariance, where harmonic dependence of field quantities on time can be assumed.

2. THE EQUATION

For electromagnetic field problems with translational or rotational invariance, the calculations are greatly simplified by introduction of the electromagnetic potentials  $A$  and  $V$ . The system of Maxwell equations with the displacement current omitted is

$$\begin{aligned}\nabla \times \vec{H} &= \vec{i} & (1) \\ \nabla \times \vec{E} &= -\partial \vec{B} / \partial t & (2) \\ \nabla \cdot \vec{B} &= 0 & (3) \\ \nabla \cdot \vec{D} &= 0 & (4)\end{aligned}$$

for regions with no free charges. The constitutive relations are

$$\begin{aligned}\vec{B} &= \mu \vec{H} = \mu_r \mu_0 \vec{H} & (5) \\ \vec{D} &= \epsilon \vec{E} = \epsilon_r \epsilon_0 \vec{E} & (6) \\ \vec{i} &= \sigma \vec{E} & (7)\end{aligned}$$

where  $\mu$ ,  $\epsilon$ ,  $\sigma$  are the permeability, permittivity, and conductivity, respectively. The introduction of the vector potential by  $\vec{B} = \nabla \times \vec{A}$  and of the scalar potential by  $\vec{E} + \partial \vec{A} / \partial t = -\nabla V$  together with the choice of the Coulomb (or radiation) gauge  $\nabla \cdot \vec{A} = 0$  yields the equations

$$\begin{aligned}\nabla \times \left( \frac{1}{\mu} \nabla \times \vec{A} \right) + \sigma \partial \vec{A} / \partial t &= \sigma (-\nabla V) & (8) \\ \nabla \cdot (\epsilon \nabla V) &= 0 & (9)\end{aligned}$$

In this gauge,  $-\nabla V$  acts as a source of the  $\vec{A}$ -field and  $V$  can be identified with the applied potential. If  $V$  is known, we do not have to solve eq. (9).

For a problem with translational invariance along the Cartesian  $z$ -axis,  $\vec{A}$  has only one component,  $A = A_z(x, y, t)$ . Eq. (8) the reduces to

$$-\nabla \cdot \left( \frac{1}{\mu} \nabla A \right) + \sigma \partial A / \partial t = \sigma (-\nabla V) \quad (10)$$

When the material properties  $\mu$  and  $\sigma$  are time- and field-independent,  $A$  and  $V$  will have the same time dependence. If it is sinusoidal,  $A = A_0(x, y)e^{j\omega t}$ ,  $V = V_0(x, y)e^{j\omega t}$ , then (10) simplifies to

$$-\nabla \cdot \left( \frac{1}{\mu} \nabla A_0 \right) + j\omega A_0 = \sigma (-\nabla V_0) \quad (11)$$

This equation is sometimes called the diffusion equation.  $(-\nabla V_0)$  can be identified for each conductor with the voltage (in V/m) applied to it.

Similar relations can be worked out for axisymmetric problems.

3. BOUNDARY CONDITIONS

Boundary conditions for the vector potential can be of two types. Either can the magnetic "reluctance"  $\alpha$  be specified along a boundary

$$\hat{n} \times \vec{H} = \hat{n} \times \left( \frac{1}{\mu} \nabla \times \vec{A} \right) = \alpha (\vec{A}_g - \vec{A}) \quad (12)$$

or the vector potential can be specified there

$$\vec{A} = \vec{A}_g \quad (13)$$

where  $g$  stands for "given". The special case of condition (12) with  $\alpha=0$  corresponds to insulation or symmetry, the special case of condition (13) with  $\vec{A}_g = 0$  corresponds to antisymmetry along the boundary

4. CONSTRAINTS

Frequently, one knows the total current carried by a group of conductors in parallel rather than the applied voltage. Then the following constraint must be satisfied:

$$\bar{J}_i^{\text{tot}} = \int_{\Omega_i} \sigma (-\nabla V - \partial \bar{A} / \partial t) \, d\Omega_i \quad (14)$$

where the integration area  $\Omega_i$  is a cross-section of the  $i$ :th conductor group. If there is only one such group, the problem can first be solved for a unit applied voltage and the corresponding total current  $J_1$  is determined. The proper voltage can be determined by the principle of superposition, by simply computing the ratio  $J^{\text{given}} / J_1$ . More generally, the principle of superposition may be applied when a system of conductor groups with specified total currents is given, leading to the computation of an admittance matrix. The proper voltages can then be obtained with the aid of this matrix.

Another possible constraint can emerge when one has a prohibitively large number of conductors close to each other, as in a coil, where the skin-effect is unimportant. In order to bring down the computing costs, one would like to treat all of these conductors together, requesting constant current density across the coil. Rather than eq. (8), one has in this area

$$\nabla \times \left( \frac{1}{\mu} \nabla \times \bar{A} \right) = \bar{J}^{\text{given}} \quad (15)$$

Then, different equations ((8) or (15)) apply in different parts of the domain of computation.

#### 5. THE F.E.M.

Eq. (11) can be written in the form

$$DA = b \quad (16)$$

where the differential operator  $D = -\nabla \cdot \frac{1}{\mu} \nabla + j\omega\sigma$  is not self-adjoint. An approximation  $A_1$  to  $A_0$  is sought of the form

$$A_1 = \sum_{i=1}^N \alpha_i \psi_i, \quad (17)$$

where the  $\psi_i$  are real polynomials,  $\alpha_i$  are their complex weights and  $N$  is the number of nodes in the F.E. mesh.  $A_1$  is required to obey the Galerkin condition

$$(\psi_k, DA_1 - b) = 0 \quad k=1, \dots, N \quad (18)$$

Thus a system of algebraic equations is obtained, which can be solved by some standard method. The heart of every computer program using the F.E.M. lies of course here and the task of constructing a fast solver with reasonable memory requirements is a most challenging one.

#### 6. ECSTASy

A F.E. computer program named ECSTASy (Eddy Currents & Skin effect Twodimensional Analysis System) solving eq. (8) for cases with translational or rotational invariance has been developed at the KDT-department of the ASEA Company in Västerås, Sweden. It uses triangular elements and the approximating polynomial can be of the 1:st to the 5:th degree. ECSTASy uses a direct method for solving the equation system. External memory (disc) is used during matrix factorization and back-substitution in order to bring down the memory requirements.

ECSTASy consists of 150 FORTRAN subroutines. A separate preprocessor is used for triangulation. A digitizer can be used for generation of input data. A postprocessor named PostECSTASy analyses the results, integrates the current, induced current, ohmic losses, reactive effect, magnetic energy, Maxwell stresses, and plots the isolines for ohmic losses and real part of the vector potential for different points of time.

ECSTASy requires 35K 36-bit words on a Honeywell Bull 6080 computer. The memory requirements can be illustrated by a couple of examples: A problem with 200 elements and polynomial degree 3 having about 1000 complex unknowns requires 64K in the core, the program included. A problem with 800 elements and solution degree 2 having 1700 complex unknowns would require about 75K words.

An example of a field plot is shown below. The device is a continuous casting mould stirrer. Four coils with applied voltages with a relative phase shift  $90^\circ$  create a rotating field. The plotted lines represent the equipotential lines of the real part of the vector potential at the beginning of each period.





# FREDHOLM INTEGRAL EQUATIONS FOR THREE AND TWO-DIMENSIONAL EDDY CURRENT PROBLEMS

J. H. McWhirter  
WESTINGHOUSE R&D CENTER, PITTSBURGH, PA 15235, U. S. A.

R. C. MacCamy  
CARNEGIE-MELLON UNIVERSITY, PITTSBURGH, PA 15213

## ABSTRACT

This paper is a discussion of the Fredholm integral equations which govern the induction of current in conductors for the following types of problems: (1) general three-dimensional, (2) three-dimensional with thin conductors, and (3) two-dimensional with current parallel to the z axis. A description is given of a computer code implementing the two-dimensional equation with the inclusion of prescribed boundary and interface conditions. By limiting approximate solutions to those which have no conductor current normal to the conductor surface and using an inner product procedure (the method of moments), equations are provided which do not have a term involving surface charge.

## INTRODUCTION

### Background

Eddy current problems have been solved analytically<sup>1, 2</sup> and numerically<sup>3-6</sup> using the two-dimensional diffusion equation. Recent work<sup>7, 8</sup> on the numerical solution of three-dimensional problems have shown the need for conductor surface charges in order to obtain mathematical consistency. In general, these surface charges are also necessary in problems with two-dimensional geometry, causing the solution to not be two-dimensional.

This paper discusses a Fredholm integral equation formulation of the three-dimensional eddy current problem. The physical meaning and importance of the surface charge is discussed. An inner product or method of moments<sup>11</sup> procedure (e.g., Galerkin's method) is shown to provide an approximation which does not include surface charge effects. The general three-dimensional equation is specialized to a problem where the conductor is thin in one dimension, but still three-dimensional. Also, the two-dimensional equation with z directed currents is formulated. This two-dimensional equation has been implemented in a computer code<sup>6</sup> called FREDDY which also permits several types of prescribed boundary and permeability interface

conditions, as well as fixed sources. The solution of a problem demonstrates the effectiveness of the code.

This paper (a) contributes to a physical understanding of surface charge, (b) provides a mathematical rationalization for the elimination of this surface charge from several two- and three-dimensional Fredholm integral equations, and (c) demonstrates the application of the two-dimensional equation on a problem involving permeability interfaces and fixed current sources.

Throughout this paper, we deal with the phasor representation of steady state quantities which are sinusoidal in time. We have in mind problems where the frequencies are about 50-60 Hz and problem dimensions are about 10 meters or less.

## BASIC DISCUSSION

Currents in a conducting body are a consequence of an electric field  $E$  and Ohm's Law,  $J = \sigma E$ . The electric field, in an engineering sense, may result from (1) a changing magnetic field caused by current in another body (Fig. 1a), (2) an electric field caused by external charges (Fig. 1b), or (3) a connected source of voltage (Fig. 1c). In general, these currents imply a difference

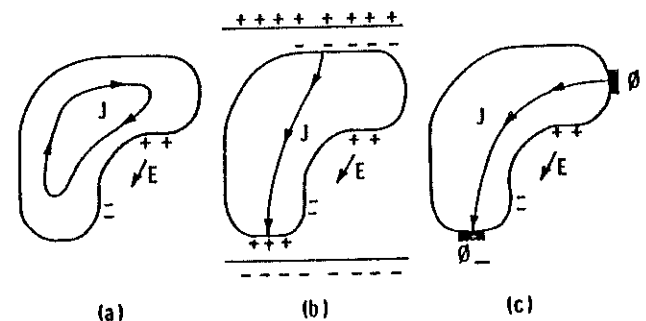


Fig. 1 - Several modes of current induction

in potential between various parts of the conductor surface and an electric field external to the conductor. If we apply Gauss's law (or  $\nabla \cdot E = \rho_v / \epsilon$ ) to a thin disk enclosing the surface shown in Fig. 2a, we equate the surface integral of the outward normal component of  $\epsilon E$  to the enclosed charge. ( $\rho_v$  is volume charge density).

$$\rho da = \epsilon(E_{no} - E_{ni})da \approx \epsilon E_{no} da \quad \text{or} \quad \rho = \epsilon E_{no} \quad (1)$$

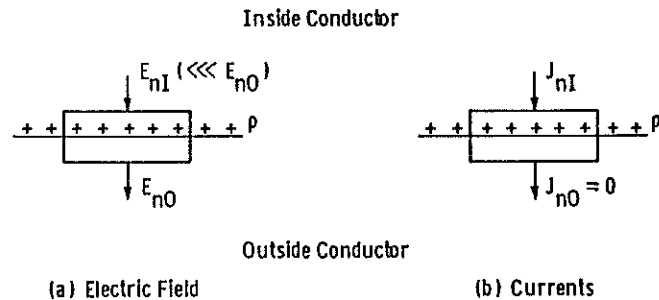


Fig. 2 - Boundary conditions on conductor

The surface integral of the outward normal component of current is equal to the time rate of change of the enclosed charge. This is the integral form of  $\nabla \cdot \underline{J} = -\frac{\partial \rho}{\partial t}$ . In Fig. 2(b), using phasor notation,

$$j\omega p da = J_{nI} da \quad \text{or} \quad J_{nI} = j\omega p \quad (2)$$

Equation 1 shows the need for a surface charge and equation 2 shows the requirement for a normal component of current at the interior surface of the conductor. We may think of equation 2 as representing capacitive or displacement current. In this sense, we have not yet neglected displacement current.

### THREE-DIMENSIONAL INTEGRAL EQUATION

Consider a conducting body with internal currents and surface charges. Assume the same permeability  $\mu$  and dielectric constant  $\epsilon$  everywhere and that  $\nabla \cdot \underline{J} = 0$  within the conductor. This model is consistent with Maxwell's equations within and outside the conductor and with the required continuities at the surface.

In general, the electric field at a point  $f$  is

$$\underline{E}(f) = -j\omega \underline{A}(f) - \nabla \phi(f) \quad (3)$$

where the vector potential  $\underline{A}$  results from currents and the scalar potential results from charges. In our problem, this becomes

$$\underline{E}(f) = -\frac{j\omega\mu}{4\pi} \int_V \underline{J}(s) G(f,s) dv - \frac{1}{4\pi\epsilon} \nabla \int_S \rho(s) G(f,s) ds + \underline{E}_0(f) \quad (4)$$

where  $\underline{J}(s)$  is the conduction current density within the conductor,

$\rho(s)$  is the charge density on the conductor surface,

$\underline{E}_0(f)$  is the electric field at  $f$  due to external currents and charges,

$G(f,s)$  is  $(e^{j2\pi r/\lambda})/r$

$r$  is the distance from current or charge source point  $s$  to the field point  $f$ ,

$\lambda$  is the wavelength at  $\omega$ , in our case, about 5000 kilometers.

Since  $r/\lambda$  is about  $10^{-6}$ ,  $G$  can be closely approximated by  $1/r$ .

We can also write an equation for use in calculating the magnetic field after the currents have been determined:

$$\underline{B}(f) = -\frac{\mu}{4\pi} \int_V \underline{J}(s) \times \nabla G dv + \underline{B}_0(f) \quad (5)$$

Equations 4 and 5 involve basic relationships between the electric field and the currents and charges. See Stratton<sup>10</sup>, for example.

Internal to the conductor, from equation 4 and Ohm's law, the following equation holds.

$$\underline{J}(p) + \frac{j\omega\mu\sigma}{4\pi} \int_V \underline{J}(s) G(p,s) dv + \frac{\sigma}{4\pi\epsilon} \nabla \int_S \rho(s) G(p,s) da = \sigma \underline{E}_0(p) \quad (6)$$

If the term involving charge were not present, this would be an integral equation of the second kind or a Fredholm integral equation. A solution to equation 6 requires the simultaneous solution of the field equations inside and outside the conductors.

### Inner Product Approximation

If the total current density is large compared to the surface displacement current density, a solution which approximates the true solution but does not include the displacement current (or surface charge) may be sufficient. Since this approximate solution is not a solution to equation 6, we define the sense in which it is an approximation by means of an inner product. Harrington<sup>11</sup> calls this the method of moments and his discussion is valuable. Most, if not all, numerical solutions to field equations can be viewed as the application of the method of moments.

In order to make the approach clear, consider a specific finite element within the volume. Divide the conducting volume into tetrahedra. Define an electric<sup>9</sup> (or current<sup>12</sup>) vector potential  $\underline{T}$  which is piecewise linear over the volume and zero on the surface.  $\underline{T}$  is defined such that

$$\nabla \times \underline{T} = \hat{\underline{J}} \quad (7)$$

A consequence of this definition, by a vector identity, is that  $\nabla \cdot \hat{\underline{J}} = 0$  within  $V$ . If  $\underline{T}$  is zero on the surface, then  $\hat{\underline{J}} \cdot \underline{n} = 0$  on the inside of the surface.  $\hat{\underline{J}}$  is the desired approximation to  $\underline{J}$ .

Now, returning to a more general discussion, define an inner product

$$\langle \underline{u}(p), \underline{f}(\hat{\underline{J}}(s)) \rangle = \int_V \underline{u}(p) \cdot \underline{f}(\hat{\underline{J}}(s)) dv, \quad (8)$$

where  $\underline{u}$  has the properties

$$\nabla \cdot \underline{u} = 0 \quad \text{within } V$$

$$\underline{u} \cdot \underline{n} = 0 \quad \text{on } S_0, \text{ a part of } S \text{ such that } S = S_0 + S_+ + S_-.$$

We apply this inner product to equation 6. Let us examine in detail the term involving charge:

$$\frac{\sigma}{4\pi\epsilon} \int_V \underline{u}(p) \cdot [\nabla \int_S \rho(s) G(p,s) ds] dv = \sigma \int_V \underline{u}(p) \cdot \nabla \phi(p) dv \quad (9)$$

(the surface integral is the potential  $\phi(p)$  due to the surface charge distribution). By the divergence or Gauss's Theorem

$$\int_V \nabla \cdot (\phi \underline{u}) = \int_S \phi \underline{u} \cdot \underline{n} da. \quad (10)$$

By a vector identity, this is also equal to

$$\int_V \underline{u} \cdot \nabla \phi dv + \int_V \phi \nabla \cdot \underline{u} dv. \quad (11)$$

Then, equation 9 becomes

$$\sigma \int_V \underline{u} \cdot \nabla \phi dv = \sigma \int_S \phi \underline{u} \cdot \underline{n} da - \sigma \int_V \phi \nabla \cdot \underline{u} dv \quad (12)$$

We assume that  $\phi$  is constant at  $\phi_+$  over  $S_+$  and constant at  $\phi_-$  over  $S_-$ .

Since  $\nabla \cdot \underline{u} = 0$  within  $V$ , the second term is zero. Since  $\underline{u} \cdot \underline{n} = 0$  on  $S$  excepting  $S_+$  and  $S_-$ , the remaining terms are

$$\sigma \int_{S_+} \phi_+ \underline{u} \cdot \underline{n} da + \sigma \int_{S_-} \phi_- \underline{u} \cdot \underline{n} da = -\sigma (\phi_+ U_{n+} + \phi_- U_{n-}) \quad (13)$$

where  $U_n = - \int_S \underline{u} \cdot \underline{n} da$ .

Equation 6 becomes

$$\int_V \underline{u}(p) \cdot \hat{\underline{J}}(p) dv_p + \frac{j\omega\mu\sigma}{4\pi} \int_V \underline{u}(p) \cdot [\int_V \hat{\underline{J}}(s) G(p,s) dv_s] dv_p = \sigma (\phi_+ U_{n+} + \phi_- U_{n-}) + \sigma \int_V \underline{u}(p) \cdot \underline{E}_0(p) dv_p \quad (14)$$

The two terms on the right-hand side respectively represent the driving force from an applied potential and the driving force induced by charges or currents located elsewhere.

In a numerical solution

$$\hat{\underline{J}}(s) = \sum_n \hat{\underline{J}}_n(s) = \sum_n \alpha_n \underline{f}_n(s) \quad n = 1, M \quad (15)$$

$$\underline{u}(p) = \underline{u}_m(p) \quad m = 1, M$$

where  $\underline{f}_n$  are basis functions derived from the piecewise linear basis functions for

$$\underline{T}_n = T_n \underline{t}_n(s). \quad (16)$$

Using the method described by Harrington, this becomes a matrix equation

$$[L_{mn}] [\alpha_n] = [g_m] \quad (17)$$

where

$$L_{mn} = \int_V \underline{u}_m(p) \cdot \underline{f}_n(s) dv_p \quad \text{and} \quad (18)$$

$$g_m = \sigma \int_V \underline{u}_m(p) \cdot \underline{E}_0(p) dv_p + \sigma(\phi_+ U_{n+} + \phi_- U_{n-}) \quad (19)$$

#### THIN CONDUCTORS

Consider a conductor which is thin (e.g., sheet aluminum) and is formed into a complex curved shape. Equation 14 can be written for this problem by considering that points  $p$  and  $s$  lie on the surface  $S'$  midway between the conductor surfaces. We assume that the current density does not vary appreciably through the thickness. We define our approximate solution  $\hat{\underline{J}}$  and the weighting function  $\underline{u}$  to be constant in the thickness direction. Then, equation 14 becomes

$$\begin{aligned} \int_{S'} \underline{u}(p) \cdot \hat{\underline{J}}(p) da_p + \frac{j\omega\mu\sigma h(p)}{4\pi} \int_{S'} \underline{u}(p) \cdot \left[ \int_{S'} \underline{I}(s) G(p,s) da_s \right] da_p \\ = \sigma(\phi_+ U_{n+} - \phi_- U_{n-}) + \sigma h(p) \int_{S'} \underline{u}(p) \cdot \underline{E}_0(p) da_p \end{aligned} \quad (20)$$

where

$$\hat{\underline{I}}(p) = \hat{\underline{J}}(p)h(p) \quad (\text{Amperes per unit length})$$

$h(p)$  is the thickness of the conductor at point  $p$  on the midsurface.

The basis functions for  $\underline{u}$  and  $\underline{J}$  are chosen with the restriction that their normal components at edges be zero and their two-dimensional divergence be zero. We can define a vector function  $\underline{T}$  in the plane  $S'$  such that

$$\begin{aligned} T_{t1} &= T_{t2} = 0 \\ T_n &= \psi \end{aligned}$$

where  $T_{t1}$  and  $T_{t2}$  are the magnitudes of  $\underline{T}$  in the two-orthogonal directions  $t_1$  and  $t_2$  which are tangent to  $S'$ .  $T_n = \psi$  is the magnitude of  $\underline{T}$  in the direction normal to  $S'$ .

If  $\hat{\underline{I}} = \nabla \times \underline{T}$  then

$$\begin{aligned} \hat{I}_{t1} &= \frac{\partial \psi}{\partial t_2} \quad \text{and} \\ \hat{I}_{t2} &= -\frac{\partial \psi}{\partial t_1} \end{aligned}$$

If  $\psi$  is zero on the conductor edges, there is automatic assurance that the normal component of  $\hat{\underline{I}}$  equal 0. The function  $\underline{u}$  can also be defined as a curl, thus assuring that  $\nabla \cdot \underline{u} = 0$  and that the component of  $\underline{u}$  normal to the boundary is zero.

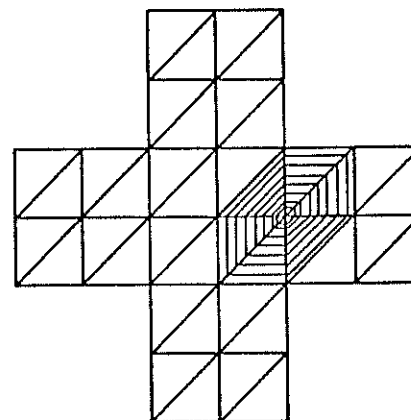


Fig. 3 - Finite elements and  $\psi$  basis function for thin conductor

If  $S'$  is divided into triangular finite elements as shown in Fig. 3 and  $\psi$  is piecewise linear over each triangle, the current components  $\hat{I}_{t1}$  and  $\hat{I}_{t2}$  will be piecewise constant.  $\psi$  is a linear combination of basis functions each of which is linear over the triangles having a common vertex and zero over all other triangles. The lines in Fig. 3 which resemble a spider's web can be regarded as contours of  $\psi$  or as lines of current flow for one of the basis functions.

If  $\hat{f} = \sum_n \alpha_n \underline{f}_n$  and

$$\underline{u}_m = \underline{f}_m,$$

the solution is by Galerkin's method. If  $\underline{u}(p) = (\underline{t}_1 + \underline{t}_2) \delta(q-p)$ , the solution is by point matching where  $\underline{t}_1$  and  $\underline{t}_2$  are unit vectors. The Dirac delta function  $\delta(q-p)$  is defined as

$$\delta(q-p) = \begin{cases} 0 & q \neq p \\ \infty & q = p \end{cases}$$

$$\int_S \delta(q-p) da = 1$$

## TWO-DIMENSIONAL PROBLEMS

We wish to find approximate solutions  $\hat{j}$  which have only an axial or  $z$  component and which are invariant in  $z$  over a length  $L$ . Therefore, we choose weighting functions and solution functions which have these properties. Then, equation 14 becomes

$$\int_A \underline{u}(p) \hat{j}(p) dx_p dy_p + \frac{j\omega\mu\sigma}{4\pi} \int_A \underline{u}(p) \left[ \int_A \hat{j}(s) G_2(p,s) dx_s dy_s \right] dx_p dy_p = \sigma(\phi_{+U_{n+}} + \phi_{-U_{n-}})/L + \sigma \int_A \underline{u}(p) E_o(p) dx_p dy_p \quad (21)$$

$$\text{where } G_2(p,s) = \int_L G(p,s) dz_s \quad \text{and}$$

$\underline{u}(p)$  = the  $z$  component of  $\underline{u}(p)$ ; etc., for other previously defined vector quantities.

If  $L$  is infinite

$$G_2(p,s) = -\ln r(p,s).$$

If we define  $\underline{u}(p)$  as a Dirac delta function  $\delta(q-p)$  where

$$\delta(q-p) = \begin{cases} 0 & \text{if } p \neq q \\ \infty & \text{if } p = q \end{cases}$$

$$\int_A \delta(q-p) da_p = 1$$

equation 21 becomes

$$\hat{j}(q) + \frac{j\omega\mu\sigma}{4\pi} \int_A \hat{j}(p) G_2(q,p) dx_p dy_p = \sigma(\phi_{+} - \phi_{-})/L + \sigma E_o(q) \quad (22)$$

This equation is consistent with traditional eddy current analyses. As  $\omega$  approaches zero, equation 22 approaches the correct direct current equation.

## DISCUSSION OF BOUNDARY CONDITIONS

Boundaries with prescribed conditions, such as tangential  $\underline{B}$  or a discontinuity in normal  $\underline{H}$ , may be replaced by layers of equivalent sources. These boundary conditions can be formulated as integral equations of the second kind or Fredholm integral equations. These have been worked out in detail for two-dimensional problems<sup>6</sup> and implemented in a computer code. In the case of permeability interface and prescribed value of tangential  $\underline{B}$ , the equivalent source is a layer of  $z$  directed current at the boundary. Other equivalent sources are appropriate in three dimensions, but a discussion of this is beyond the scope of this paper.

## EXAMPLE OF TWO-DIMENSIONAL SOLUTION

There is a two-dimensional computer code called FREDDY<sup>6</sup> which incorporates equation 21 and other equations for various boundary conditions. This code has been used to compute the magnetic field and the eddy currents for the problem of Fig. 4. This is a conducting channel with a square cross-section and a current dipole with a magnitude of  $1. \times 10^5$  ampere-cm. at the center. The relative permeability of the channel is 25 and the resistivity is  $59.22 \times 10^{-6}$  ohm-cm. The outside dimension of the channel is 28 cm, and the wall thickness is 4 cm or 4 skin depths. The frequency is 60 Hz. The loss densities as a function of a perimeter distance are plotted in Fig. 5. This code approximates the  $z$  directed currents as being confined to lines in the cross-sections of Fig. 4.

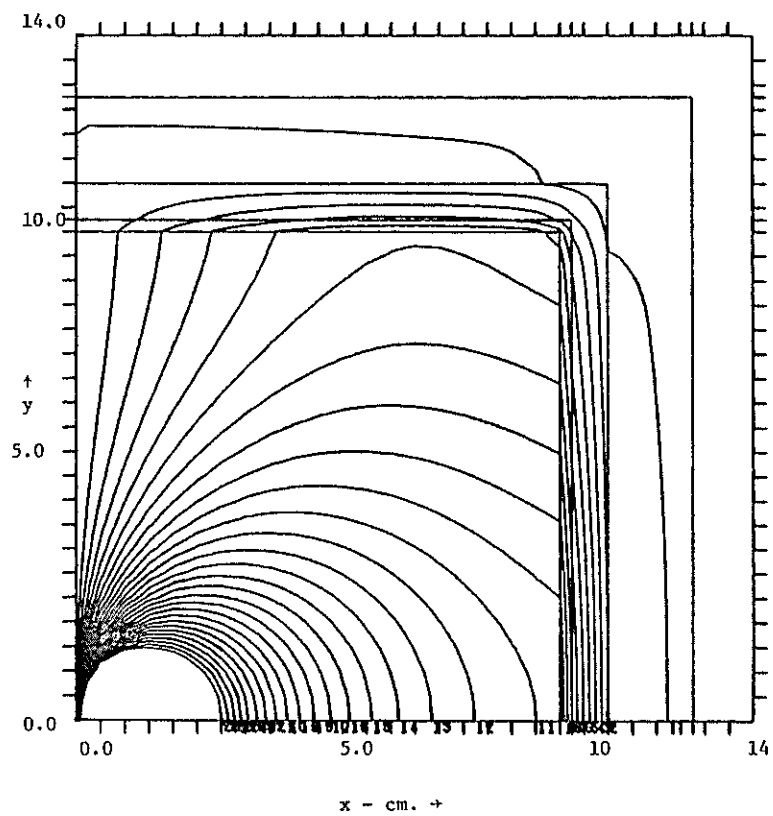


Fig. 4(a) - Real Flux Pattern

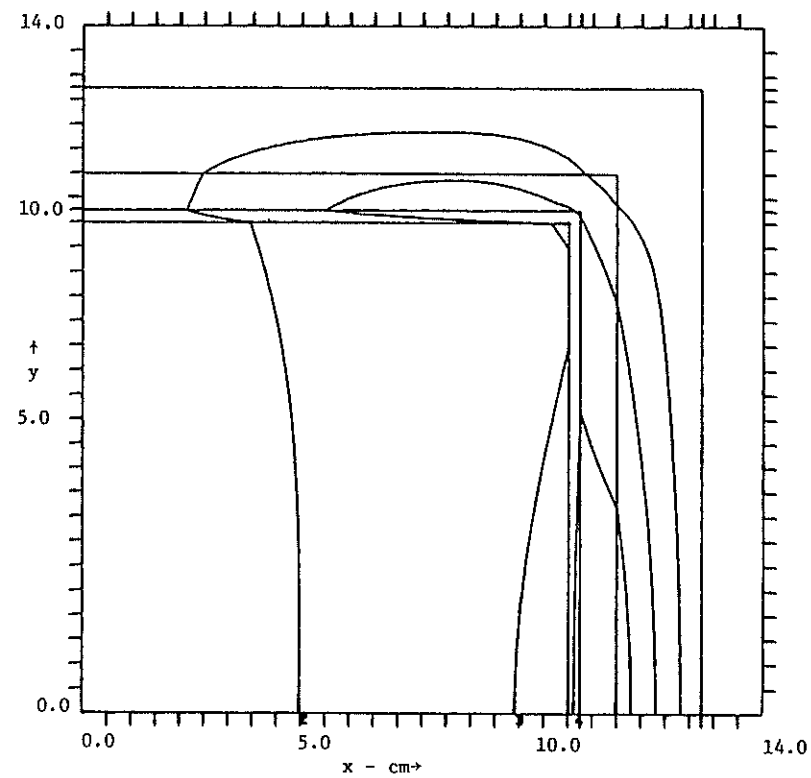


Fig. 4(b) - Imaginary Flux Pattern

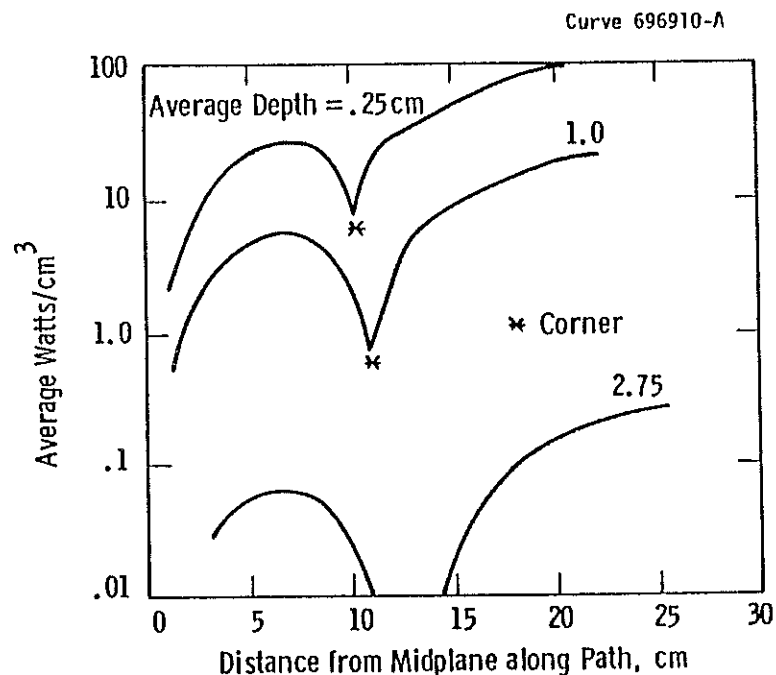


Fig. 5 - Loss Distribution in Conducting Channel  
at Several Depths into Conductor

#### DISCUSSION

The use of the inner product to produce an equation not involving surface charge may be viewed with suspicion as to its interpretation by some and regarded as completely unnecessary by others. Often it has been stated that "we neglect displacement current." This quick disposal of the charge problems does not provide the understanding, in the view of the writer, that the foregoing discussion does. It is also unsatisfactory to a careful, mathematically-oriented analyst. Another possible approach might be to let the frequency become very small and disregard some higher order terms; not so far, however, as to proceed to the dc situation. Setting the dielectric constant of the non-conducting space to zero should also eliminate the surface charge from consideration. The writers have not worked out the mathematics of these last two approaches.

#### REFERENCES

1. R. L. Stoll, The analysis of eddy currents, Clarendon Press, Oxford, 1974.
2. W. R. Smythe, Static and Dynamic Electricity, McGraw-Hill, New York, 1968.
3. P. Silvester, Skin effect in multiple and polyphase conductors, IEEE Trans., Vol. PAS-88, No. 3, 1969.
4. C. J. Carpenter, Computation of magnetic fields and eddy currents, 5th Int. Conf. on Magnetic Technology. Rome, 1975.
5. O. W. Anderson, Finite element solution of skin effect and eddy current problems, IEEE PES paper A77 616-6, July, 1977.
6. J. H. McWhirter, R. J. Duffin, P. F. Brehm, and J. J. Oravec, A computational method for solving static field and eddy current problems via Fredholm integral equations, submitted to IEEE Magnetics Society, 1978.
7. R. J. Mac Camy and J. H. McWhirter, Eddy currents in thin sheets, WFPS TCTR 227, Westinghouse Electric Corporation, Large, PA, 1976.



8. C. S. Biddlecombe, C. J. Collie, J. Simkin, C. J. Trowbridge, The integral equation method applied to eddy currents, Proc. COMPUMAG Conference on the Computation of Magnetic Fields, Oxford, 1976.
9. C. J. Carpenter and D. H. Locke, Numerical models of three-dimensional end winding arrays, Proc. COMPUMAG Conference on the Computation of Magnetic Fields, Oxford, 1976.
10. J. A. Stratton, Electromagnetic Theory, McGraw-Hill, New York, 1941, equations 19 and 20, Section 8.14, p. 466.
11. R. F. Harrington, Field computation by moment methods, The Macmillan Company, New York, 1968.
12. J. H. McWhirter and M. W. Thomas, Eddy current losses in conducting slabs, IEEE Trans. 71TP208-PWR, 1971.

# CALCULATION OF EDDY-CURRENTS INDUCED IN THIN CURVED SHEETS

M. Gramz, J. Purczyński, R. Sikora  
Polytechnic of Szczecin, Poland

## ABSTRACT

The paper deals with a method for calculating of eddy-currents induced in a thin conducting curved sheet placed in an alternating magnetic field. Two scalar potentials are introduced to formulate field equations. The method is demonstrated by examples of a spherical cap placed in alternating magnetic field and a disk rotating in magnetic field. Some numerical results are given to compare the method proposed with previously used one.

## 1. INTRODUCTION

It has been shown in Reference 1 that the formulation of the electromagnetic field equations assumes some importance when 3-dimensional eddy current problems are considered and the most familiar formulation in terms of the magnetic potential  $A$  becomes inconvenient for the numerical treatment. The alternative ways in which the eddy current problems can be described have been discussed in References 1,2,7 where the electric vector potential  $T$  and magnetic scalar potential  $\Omega$  have been used.

The purpose of the paper is to examine a method of field equations formulation in the particular case when the conducting region has a form of an infinitesimal thin curved sheet. In this case further simplifications are possible. A number of different workers 3,5,6,7,8 have investigated this problem under the following assumptions:

- 1<sup>o</sup> the thickness  $d$  of the conducting plate is much more smaller than a depth of penetration of the electromagnetic wave,
- 2<sup>o</sup> the secondary magnetic field due to eddy-currents is negligible comparing with the exciting flux.

There are however a lot of devices which often occur in electric machines and instruments where demagnetizing flux produced by eddy-currents is comparable with the exciting magnetic field and the assumption 2<sup>o</sup> is not reasonable. Taking into account the demagnetizing flux the field equations can be formulated in terms of current flow function  $I$  and magnetic scalar potential  $\Omega$ . The formulation proposed is similar to that in terms of electric vector potential  $T$ , but it leads to simpler equations and interface conditions.

## 2. FIELD EQUATIONS

Let consider a thin curved sheet of uniform thickness  $d$ , made of a conducting material having the conductivity  $\gamma$ . We assume that the thickness of the sheet is infinitesimal,  $d \rightarrow 0$ , and the conductivity of the conductor is infinite,  $\gamma \rightarrow \infty$ , but  $\lim \gamma \cdot d = \sigma < \infty$ .

The sheet is placed in an alternating magnetic field  $\vec{H}_w(t)$  and eddy currents are induced in it. To formulate equations describing the phenomenon current flow function  $I$  and magnetic scalar potential  $\Omega$  are applied. We chose an appropriate curvilinear coordinate system  $(u_1, u_2, u_3)$  in which the sheet under investigation can be described as a surface  $S : u_1 = \text{const.}$ ,  $f(u_2, u_3) < G$  with the boundary  $\Gamma : f(u_2, u_3) = G$  /Fig.1/.

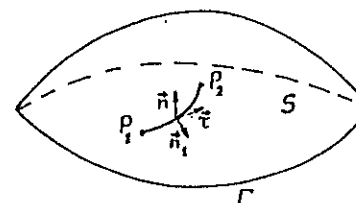


Fig.1 Thin curved sheet under investigation.

Since current density  $\vec{j}$  is infinite in the region  $S$  the surface current density  $\vec{K}$  is used:

$$\vec{K} = \lim \vec{j} d \quad (1)$$

Let introduce current flow function  $I$  defined by the equation:

$$\vec{K} = - \vec{n} \times \text{grad } I \quad (2)$$

where  $\vec{n} = \vec{e}_{u_1}$  denotes unit vector normal to the surface  $S$ . This definition is based on the similar one given in References 3,5,6,7. Current flow function  $I$  is related in a simple way to the current  $\mathcal{I}$  flowing between two arbitrary points  $P_1$  and  $P_2$  lying on the surface  $S$ :

$$\begin{aligned} \mathcal{I} &= \int_{P_1 P_2} \vec{K} \cdot \vec{n}_1 dl = - \int_{P_1 P_2} (\vec{n} \times \text{grad } I) \cdot \vec{n}_1 dl = \int_{P_1 P_2} (\text{grad } I) \cdot \vec{r} dl = \\ &= I(P_1) - I(P_2) \end{aligned}$$

The above yields the boundary condition for the  $I$  function:  $I = 0$  at  $\Gamma$ .

In order to describe secondary magnetic field generating by the eddy-currents, the scalar magnetic potential  $\Omega$  is introduced:

$$\vec{H} = - \text{grad } \Omega \quad (3)$$

which satisfies Laplace's equation

$$\nabla^2 \Omega = 0 \quad (4)$$

everywhere except on the surface  $S$ , where it is discontinuous.

The magnetic field at the surface  $S$  is described by the relations:

$$\vec{n} \times (\vec{H}_+ - \vec{H}_-) = \vec{K} \quad (5)$$

$$\vec{n} \cdot \vec{B} = 0 \quad (6)$$

where  $\vec{H}_+$  and  $\vec{H}_-$  are magnetic intensity vectors on the upper and lower side of the surface respectively.

Applying (2) and (3) we obtain

$$-\vec{n} \times \text{grad } \Delta \Omega = -\vec{n} \times \text{grad } I \quad (7)$$

and taking into account the properties of the  $I$  and  $\Omega$  functions

$$\Delta \Omega = I \quad (8)$$

what gives the boundary condition for the eqn. (4).

From the Faraday law it results

$$\text{curl}_n \vec{K} = -\epsilon \frac{\partial B_n}{\partial t} \quad (9)$$

After substituting for  $\vec{K}$  and  $B_n$  eqn. (9) takes the form

$$\text{curl}_n (\vec{n} \times \text{grad } I) = \epsilon \mu \left( \frac{\partial H_{wn}(t)}{\partial t} - \frac{\partial^2 \Omega}{\partial n \partial t} \right) \quad (10)$$

which can be written explicitly in curvilinear coordinates system  $(u_1, u_2, u_3)$  as follows

$$\frac{1}{h_2 h_3} \left[ \frac{\partial}{\partial u_2} \left( \frac{h_3}{h_2} \frac{\partial I}{\partial u_2} \right) + \frac{\partial}{\partial u_3} \left( \frac{h_2}{h_3} \frac{\partial I}{\partial u_3} \right) \right] = \epsilon \mu \frac{\partial}{\partial t} \left( H_0 - \frac{1}{h_1} \frac{\partial \Omega}{\partial u_1} \right) \quad (11)$$

where  $h_1, h_2, h_3$  are appropriate metric coefficients and  $H_0 = \vec{n} \cdot \vec{H}_w$ .

Equations (4) and (11) accompanied by the boundary conditions form a system of partial differential equations which is to be solved.

It is worth noting that the method proposed is related in a simple way to the method applied in the references 3, 5, 6, 8. If the magnetic field due to eddy currents is negligible comparing with the exciting field, the homogenous Dirichlet problem should be solved for equation (11) in which the term

$\frac{1}{h_1} \frac{\partial \Omega}{\partial u_1}$  is omitted.

On the other hand the secondary magnetic field may cancel the exciting field at the sheet surface and the problem is then to solve Laplace equation (4) accompanied by Neumann boundary condition

$$\frac{\partial \Omega}{\partial n} = H_0 \quad (12)$$

### 3. SPHERICAL CAP IN ALTERNATING MAGNETIC FIELD

To demonstrate the method proposed let consider an example of conducting spherical cap placed in an uniform alternating magnetic field

$$H(t) = H\sqrt{2} \sin \omega t = \text{Im} [H\sqrt{2} e^{j\omega t}] \quad (13)$$

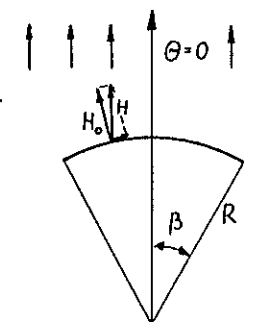


Fig.2 Spherical cap in an uniform alternating magnetic field.

The normal component of the exciting magnetic field intensity vector is

$$H_0 = H \cos \theta$$

In the spherical coordinates eqn. (4) has a solution in the form

$$\Omega_+ = \sum_{n=0}^{\infty} B_n r^{-n-1} P_n(\cos \theta) \quad r > R \quad (14a)$$

$$\Omega_- = \sum_{n=0}^{\infty} A_n r^n P_n(\cos \theta) \quad r < R \quad (14b)$$

where  $P_n(\cos \theta)$  are Legendre polynomials.

Since the normal component of the magnetic field must be continuous for  $r = R$ , we have

$$B_n = -\frac{n}{n+1} R^{2n+1} A_n$$

and

$$\Delta \Omega = \Omega_+ - \Omega_- = -\sum_{n=0}^{\infty} \frac{A_n}{n+1} R^n P_n(\cos \theta), \quad r=R \quad (15)$$

After substituting for  $\frac{\partial \Omega}{\partial r}$  eqn. (11) becomes

$$\frac{1}{R^2} \left[ \frac{d^2 I}{d\theta^2} + \cot \theta \frac{dI}{d\theta} \right] = j\omega \mu \epsilon \left( H \cos \theta - \sum_{n=0}^{\infty} n R^{n-1} A_n P_n(\cos \theta) \right) \quad (16)$$

Eqn. (16) has a solution

$$I = j\alpha \left( \frac{HR}{2} (\cos \beta - \cos \theta) - \sum_{n=0}^{\infty} a_n (P_n(\cos \beta) - P_n(\cos \theta)) \right) \quad (17)$$

where  $\alpha = \omega \mu_0 \sigma R$ ,  $a_n = \frac{\Lambda_n R^n}{n+1}$

Taking into account the relation between  $\Delta \underline{Q}$  and  $\underline{I}$  (eqn. 8), we have

$$\sum_{n=0}^{\infty} a_n P_n(\cos \theta) = \begin{cases} j \alpha \sum_{n=1}^{\infty} (a_n - \delta_{1,n} \frac{HR}{2}) (P_n(\cos \beta) - P_n(\cos \theta)), & \theta < \beta \\ 0 & \theta > \beta \end{cases} \quad (18)$$

$\delta_{1,n}$  denotes Kronecker's symbol.

In order to evaluate unknown coefficients  $a_n$  we expand the right hand side of the eqn. (18) into a series of Legendre functions. After calculations we obtain an infinite system of equations

$$\sum_{n=1}^{\infty} a_n (j \alpha K_{m,n} - \delta_{m,n}) = j \alpha \frac{HR}{2} K_{m,1} \quad m=1, 2, \dots \quad (19)$$

$$K_{m,n} = \frac{(2m+1) \sin \beta}{2(m-n)(m+n+1)} \left[ \frac{n(n+1)}{m(m+1)} P_n(\cos \beta) P_m^1(\cos \beta) - P_m(\cos \beta) P_n^1(\cos \beta) \right]$$

which in practical computations must be appropriately truncated.

The power losses can be calculated by the formula

$$P = \frac{1}{\sigma} \int_V |\underline{K}|^2 dS \quad (20)$$

which after integration by parts is of the form

$$P = - \frac{1}{\sigma} \operatorname{Re} \left[ \int_V \underline{I}^* j \alpha \left( H_0 - \frac{\partial \Omega}{\partial n} \right) dS \right] \quad (21)$$

/asterisk denotes the complex conjugate/.

The result of integration is

$$P = \frac{4\pi}{3} \omega \mu_0 R H \Im(a_1) \quad (22)$$

In special case  $\beta = \pi$ , the power losses can be expressed explicit by a simple formula

$$P = \frac{2\pi}{3} \omega \mu_0 H^2 R^3 \frac{\alpha}{1+\alpha^2} \quad (23)$$

If we assume that the magnetic field due to eddy-currents can be ignored, the power losses in a spherical cap are given by an expression

$$P = \frac{\pi}{6} \omega \mu_0 H^2 R^3 \alpha (1 - \cos \beta)^2 (2 + \cos \beta) \quad (24)$$

Substituting  $\beta = \pi$  we have

$$P = \frac{2\pi}{3} \omega \mu_0 H^2 R^3 \alpha \quad (25)$$

Comparing the expressions (23) and (25) it is evident that the assumption made in References 3, 5, 6 is valid only for  $\alpha \ll 1$ .

#### 4. DISK ROTATING IN MAGNETIC FIELD

As the second example let consider a thin conducting disk of the radius  $R$  rotating with constant angular velocity  $\omega$  in the nonuniform magnetic field. The normal component of the exciting magnetic field  $B_{en}$  is known at the disk surface

$$B_{en} = B_0(r, \varphi), \quad z=0, \quad r < R$$

For the sake of simplicity the exciting magnetic field is assumed to be constant with time. Eqn. (11) in cylindrical coordinate system  $(z, r, \varphi)$  has the form

$$\frac{\partial^2 I}{\partial r^2} + \frac{1}{r} \frac{\partial I}{\partial r} + \frac{1}{r^2} \frac{\partial^2 I}{\partial \varphi^2} = \sigma \omega \left( \frac{\partial B_0}{\partial \varphi} - \frac{\partial^2 \Omega}{\partial \varphi \partial z} \mu_0 \right) \quad (26)$$

From the symmetry with respect to the plane  $z = 0$  we have

$$\Omega = 0 \quad \text{for} \quad z = 0, \quad r > R \quad (27)$$

and from (8)

$$2\Omega_+ = I \quad \text{for} \quad z = 0_+, \quad r < R \quad (28)$$

Constraint  $I(r=R) = 0$  completes the specification of boundary conditions required for the equations system (4), (26). However we shall additionally introduce the condition

$$\Omega = 0, \quad r = a, \quad a \gg R \quad (29)$$

in order to simplify mathematical treatment of the problem.

To solve the system of eqns (4) and (26) with the boundary conditions mentioned above the following procedure has been applied:

1° Nonhomogeneous Dirichlet problem is solved for the eqn. (4) in the semi-infinite cylinder  $r < a$ ,  $z > 0$  with function  $\Omega_+(r, \varphi)$ ,  $r < R$ ,  $z=0_+$  still indefinite.

2° Homogeneous Dirichlet problem for the Poisson equation (26) is solved for arbitrary right hand side of equation.

3° Equation (28) is used for matching the solutions obtained in steps 1° and 2° of the procedure and evaluating unknown constants appearing in these solutions.

Finally the current flow function is given by the formula

$$I = \sum_{n=1}^{\infty} \sum_{k=1}^{\infty} J_n(r \cdot q_{nk}) (A_{nk} \sin n\varphi + B_{nk} \cos n\varphi) \quad (30)$$

where

$$q_{n,k} = e_{n,k} / a \quad \text{and} \quad e_{n,k} \text{ is } k\text{-th root of the}$$

Bessel function of the first kind,  $n$ -th order. Coefficients  $A_{n,k}$  and  $B_{n,k}$  are solutions of the following infinite set of equations

$$\begin{aligned} A_{nk} P(n,k) &= \sum_{p=1}^{\infty} B_{np} G(n,k,p) + F(n,k) \\ - B_{nk} P(n,k) &= \sum_{p=1}^{\infty} A_{np} G(n,k,p) - L(n,k) \end{aligned} \quad (31)$$

$$n=1,2,\dots \quad k=1,2,\dots$$

where

$$P(n,k) = \frac{a^2 q_{nk} [J_{n+1}(a q_{nk})]^2}{n \omega \sigma \mu_0 R}$$

$$G(n,k,p) = \begin{cases} \frac{1}{q_{np}^2 - q_{nk}^2} \left[ q_{nk} J_n(R \cdot q_{nk}) J_{n+1}(R \cdot q_{np}) - q_{np} J_n(R \cdot q_{np}) J_{n+1}(R \cdot q_{nk}) \right] & k \neq p \\ \frac{R}{2} \left[ J_n^2(R \cdot q_{nk}) - J_{n-1}(R \cdot q_{nk}) J_{n+1}(R \cdot q_{nk}) \right] & k = p \end{cases}$$

$$\begin{bmatrix} F(n,k) \\ L(n,k) \end{bmatrix} = \begin{matrix} R & 2\pi \\ 0 & 0 \end{matrix} \begin{bmatrix} \cos n\varphi \\ \sin n\varphi \end{bmatrix} \begin{matrix} R & 2\pi \\ 0 & 0 \end{matrix} d\varphi dr = \frac{1}{\pi n R q_{nk}} \left( \frac{J_n(R q_{nk})}{R^n} \int_0^R r^{n+1} \frac{\partial H_0}{\partial \varphi} \right) d\varphi dr - \int_0^R r J_n(r q_{nk}) \left( \frac{\partial H_0}{\partial \varphi} \right) d\varphi$$

$$\begin{bmatrix} \cos n\varphi \\ \sin n\varphi \end{bmatrix} d\varphi dr$$

In practical computations the system is truncated to a finite number of equations.

The power losses can be calculated by the formula

$$\begin{aligned} P &= \frac{\pi \sigma \omega^2 \mu_0^2 R}{2} \sum_{n=1}^{\infty} \sum_{k=1}^{\infty} n^2 \left[ B_{nk} L(n,k) - A_{nk} F(n,k) \right] - \\ &\sum_{n=1}^{\infty} \frac{\pi n}{\sigma R^{2n}} \left[ a_n^2(R) + b_n^2(R) + 2R^{2n} \int_0^R \left( a_n(r) \frac{\partial c_n(r)}{\partial r} + b_n(r) \cdot \right. \right. \\ &\left. \left. \frac{\partial d_n(r)}{\partial r} \right) dr \right] \end{aligned} \quad (32)$$

where

$$\begin{bmatrix} a_n(r) \\ b_n(r) \\ c_n(r) \\ d_n(r) \end{bmatrix} = \frac{\sigma \mu_0 \omega}{2\pi n} \int_0^r \begin{bmatrix} -\varphi^{1+n} \\ -\varphi^{1+n} \\ \varphi^{1-n} \\ \varphi^{1-n} \end{bmatrix} \int_0^{2\pi} \frac{\partial H_0}{\partial \varphi} \begin{bmatrix} \sin n\varphi \\ \cos n\varphi \\ \sin n\varphi \\ \cos n\varphi \end{bmatrix} d\varphi d\varphi$$

To compare the method proposed and the method based on the concept of current flow function I<sub>3,5,6</sub> let consider a disk rotating in the magnetic field described by the relation

$$B_0(r, \varphi) = \begin{cases} B_m \cos n\varphi & \text{if } R_1 \leq r \leq R_2 \\ 0 & \text{if } r < R_1 \text{ or } R_2 < r \leq R \end{cases}$$

The power losses have been calculated by the formula (32) and by means of the method proposed in References 3,5,6. The results shown in Figs 3 and 4 prove that

the reaction of the eddy currents on the magnetic field is negligible for  $\epsilon = n\omega\sigma\mu_0 R < 1$ . If  $\epsilon > 1$  the contribution of the eddy currents to the magnetic field must be taken into account and the method proposed in References 3,5,6 becomes useless.

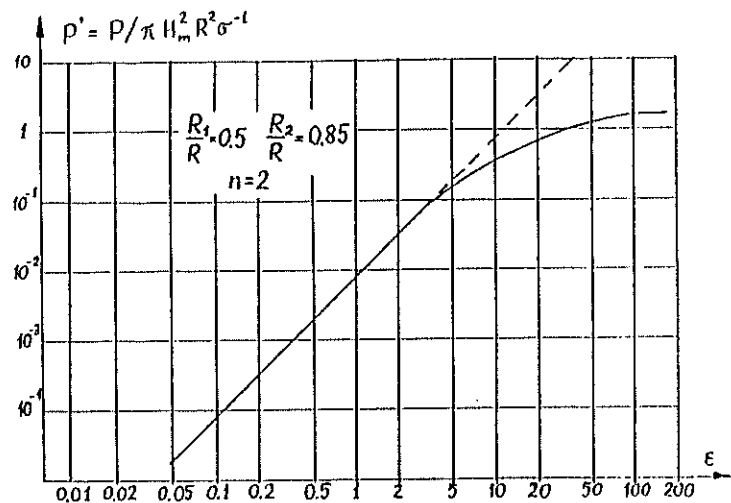


Fig. 3 Comparison between the approximate /dotted line/ and exact values of power losses as a function of an angular velocity.

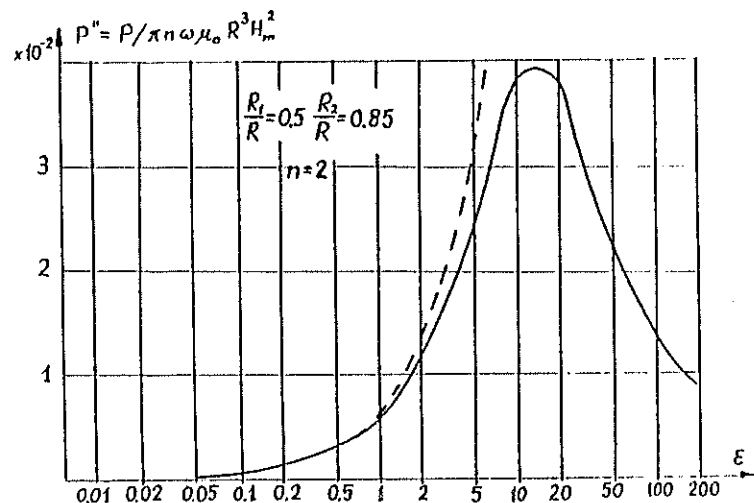


Fig. 4 Comparison between the approximate /dotted line/ and exact values of power losses as a function of a conductivity.

## 5. CONCLUSIONS

In this paper the method has been introduced allowing to take into account the secondary magnetic field due to eddy currents induced in a thin curved sheets placed in the magnetic field. The method has been demonstrated by examples and some numerical results have been provided in order to show the limitations of the method used previously.

## 6. REFERENCES

1. Carpenter, G.J. Comparison of alternative formulations of 3-dimensional magnetic-field and eddy-current problems at power frequencies. Proc. IEE, vol. 124 (1977), p.1026,
2. Carpenter, G.J. Djurovic, M. Three-dimensional numerical solution of eddy currents in thin plates. Proc. IEE, vol.122 (1975), p.684,
3. De Mey, G. A method for calculating eddy currents in plates of arbitrary geometry. Arch. f. Elektrotechn. 56 (1974) p.137,
4. Gramz, M. The calculation of eddy currents induced in a thin conductor moving with respect to the magnetic field. D.Sc. Thesis, Szczecin 1976,
5. Purczyński, J. Sikora, R., Lipiński, W. Eddy currents in thin sheets. Archiwum Elektrotechniki 21 (1972) p. 727 (in Polish),
6. Schieber, D. Unipolar induction braking of thin metal sheet. Proc. IEE vol. 119 (1972) p.1499,
7. Smythe, W.R. Static and dynamic electricity. Mc Graw-Hill Book Co. 1952,
8. Zlatev, M.P. Etude des champs électriques non potentiels. RGE 1959 nr 9.

EQUIVALENT CIRCUITS OF SOLID IRON CORE  
FOR TRANSIENT PROBLEMS

D.C. Ioan  
 Politechnical Institut of Bucharest  
 Fac. Electrotehnica, R-77206 Bucharest

## ABSTRACT

The electromagnetic circuit element is defined. In this manner is delimited the area of the electromagnetic field problems which admit electrical and/or magnetical equivalent circuits.

The dipolar magnetic circuit element with arbitrary cross-section and nonlinear B/H relationship is considered, taking into account eddy-currents. The lumped equivalent circuits has been determined for this element under small and large signal. These equivalent circuits contain ideal elements, magnetic reluctances and magnetic inductances.

The equivalent electric circuits for coils with solid ferromagnetic cores are determined. One magnetic circuit and an electric one, related with two commanded sources are suggested for this coil. Another electric equivalent circuit, dual to the magnetic equivalent circuit of the core is proposed.

## 1. INTRODUCTION

Together with the numerical and analytical methods for the solution of the electromagnetic field problems it is possible to apply the semi-analytical methods also [1]. The most important example for the semi-analytical method is the equivalent circuit technique. The main purpose of this technique is to replace transient analysis of the electromagnetic field systems by the analysis of an electric circuit. In this manner may be approach the networks which contain nonideal elements with field-effects such as eddy-currents, skin-effects.

The linear equivalent circuits for the bus-bars with skin-effect [2,3] and for the coils with solid cores [4,5,6] are known. Both devices have dipolar equivalent circuits with an infinite number of linear circuit elements R L. For the equivalent circuit synthesis, the classical Foster and Cauer's techniques has been applied from the impedance  $Z(s) = U(s)/I(s) = 1/Y(s)$ .

Using the concept of magnetic impedance  $Z_m(s) = U_m(s)/\Phi(s) = 1/Y_m(s)$ , early defined by Ekelöf [7], is possible to synthesize equivalent magnetic circuits for the dipolar magnetic devices. These circuits contain magnetic reluctances  $R_m$  and magnetic inductances  $L_m$  [8,9].

The classical synthesis techniques are no longer valid for nonlinear systems. For this reason much work is to be done in the theory of nonlinear equivalent circuits.

The purpose of this paper is to determine the equivalent magnetic circuits for the ferromagnetic cores and the equivalent electric circuits of the coils with such cores. In fact, the obtained circuits are not strict equivalent to the field systems, but they approximate these systems. For all that the results which has been obtained are more accurate than previously reported [10].

Not all electromagnetic field problems allow of equivalent circuits. A field problem may have an equivalent circuit, only if the boundary conditions make possible the connection with an external network. In this respect it is necessary to exist, on the boundary surface, some equipotential sides (the terminals) and that the electrical current to penetrate in the domain through these sides only [11].

In this paper a more general concept — the equivalent magnetic circuit element — is defined. It has electrical and/or magnetical terminals and it can be connected to an electrical and/or magnetical external network. This definition permits to delimit the area of field problems which may have equivalent circuits.

## 2. STATEMENT OF THE PROBLEM

## 2.1. Electromagnetic circuit element

It is considered a conducting domain D bounded by  $\Sigma$ . Neglecting the displacement current, the electromagnetic field equations are given by:

$$\text{curl } \vec{E} = - \frac{\partial \vec{B}}{\partial t} \quad (1)$$

$$\text{curl } \vec{H} = \vec{J} \quad (2)$$

$$\text{div } \vec{B} = 0 \quad (3)$$

with the following material relations :

$$\vec{B} = \hat{B}(\vec{H}) \quad (4)$$

$$\vec{J} = \hat{J}(\vec{E}) \quad (5)$$

Further down some useful definitions are presented.

Let  $D_x$  be a simply connected domain with regular boundary  $\Sigma$ , whose  $\Sigma$  is partitioned in  $n' + n''$  simply connected, compact, mutually disjoint sides  $S'_k (k=1, n')$ ,  $S''_k (k=1, n'')$  and an external part  $S_0$  so that  $\Sigma = S_0 \cup S'_k \cup S''_k$ .

The domain  $D_x$  is an electromagnetic circuit element if are satisfied the following conditions :

$$\vec{n} \cdot \text{curl } \vec{E}(M, t) = 0, M \in S_0 \cup S'_k \quad (6)$$

$$\vec{n} \cdot \text{curl } \vec{H}(M, t) = 0, M \in S_0 \cup S_k'' \quad (7)$$

$$\vec{n} \times \vec{E}(M, t) = 0, M \in S_k' \quad (8)$$

$$\vec{n} \cdot \vec{H}(M, t) = 0, M \in S_k'' \quad (9)$$

The sides  $S_k'$  are referred as electrical terminals and the sides  $S_k''$  are referred as magnetical terminals. On the surface  $S_0$  a set of slits  $UT_k'UT_k''$  have to be done, so that  $S_0$  into simply connected surface  $S_r$  to transform.

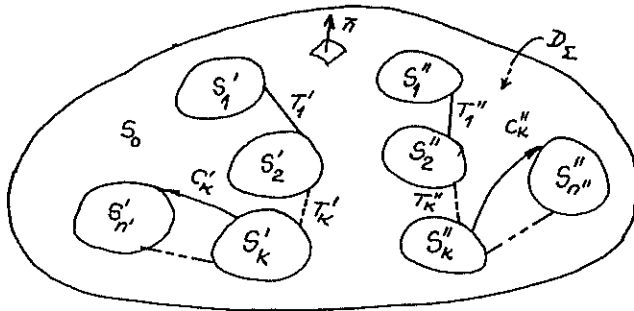


Fig.1. The electromagnetic circuit element

If an electromagnetic circuit element has only electrical terminals ( $n''=0$ ) then it is defined as an electric circuit element and if it has only magnetical terminals ( $n'=0$ ) then it is defined as a magnetic circuit element.

The conditions (6)-(9) show that the electric current penetrates in  $D_Z$  only through the electrical terminals (eqn.7), the time-varying magnetic flux penetrates in  $D_Z$  only through the magnetical terminals (eqn. 6), the electrical terminals have an electric equipotential character (eqn.8) and the magnetical terminals have a magnetic equipotential character (eqn.9).

The concept of electromagnetic circuit element allows to define the following quantities.

The electric current through the terminal  $S_k'$ :

$$i_k = \int_{S_k'} \text{curl } \vec{H} \cdot d\vec{A} \quad (10)$$

The electric potential of the terminal  $S_k'$

$$v_k = \int_{C_k' \in S_r} \vec{E} \cdot d\vec{r} \quad (11)$$

where  $C_k'$  is a curve whose start is on  $S_k'$  and whose stop is on the reference terminal  $S_n'$ .

The derivative of magnetic flux through the terminal  $S_k''$

$$\varphi_k' = \frac{d\varphi_k}{dt} = - \int_{S_k''} \text{curl } \vec{E} \cdot d\vec{A} \quad (12)$$

The magnetic potential of the terminal  $S_k''$

$$v_{mk} = \int_{C_k'' \in S_r} \vec{H} \cdot d\vec{r} \quad (13)$$

where  $C_k''$  is a curve whose start is on  $S_k''$  and whose stop is on the reference terminal  $S_n''$ .

The relations (6)-(9) guarantees the independence of the definitions (11), (13) by the choice of the curves  $C_k', C_k''$ .

As a result of (6)-(13), the defined quantities satisfy the following restrictive conditions:

$$v_{n'} = 0, v_{nn''} = 0, \sum_{k=1}^n i_k = 0, \sum_{k=1}^n \varphi_k' = 0. \quad (14)$$

The quantities (10)-(13) permit to calculate the electromagnetic power influx in the domain  $D_Z$

$$-P_Z = \int_Z (\vec{E} \times \vec{H}) \cdot d\vec{A} = \sum_{k=1}^{n'} v_k i_k + \sum_{k=1}^{n''} v_{mk} \varphi_k' \quad (15)$$

therefore these quantities determine the electromagnetic power linkage of electromagnetic circuit element with the exterior.

## 2.2. Associate system and equivalent circuits

The uniqueness theorem for the solution of the equations (1)-(9) allows to associate to any electromagnetic circuit element one input-output system [12]. This system is a nonlinear passive one and it has the vector  $v$  as the input description:

$$v = [v_1, v_2, \dots, v_{n'-1}, v_{m1}, \dots, v_{m, n''-1}]^t \quad (16)$$

and the vector  $i$  as the output description:

$$i = [i_1, i_2, \dots, i_{n'-1}, \varphi_1, \dots, \varphi_{n''-1}]^t. \quad (17)$$

The state variable of the system is the magnetic flux density  $\vec{B}(M, t), M \in D_Z$ .



Despite of finite number of the input-output variables, the system is an infinite one because the state space is infinite dimensional.

Let consider the synthesis of an equivalent multipol. This multipol must contain ideal circuit elements: resistances  $R$ , inductances  $L$ , reluctances  $R_m$ , magnetic inductances  $L_m$  and it must be equivalent, in an input-output meaning, with the electromagnetic circuit element or at least it must be the best approximation of the  $D_\Sigma$  behaviour.

The explanation of the infinite character of the equivalent circuits is related to the dimension of  $D_\Sigma$  state space. In order that, the infinite equivalent circuits, to become useful, they must be approximate by other finite circuits. Since a finite circuit is finally desired, it is normal to determine directly the approximate circuit instead of the equivalent circuit, especially for nonlinear case [12].

The equivalent circuits, in fact the best approximate circuits, are obtained using small and large signal techniques.

In small signal technique, the input is separated as  $v = v_0 + v^*$ , where  $v_0$  is the quasi-static component and  $v^*$ , the small signal component, is bounded  $\|v^*\| < M$  with  $M$  sufficiently small. The output is approximated by  $i = i_0 + i^*$ .

The static nonlinear problem (2)-(9), with

$$\text{curl } \vec{E} = 0 \quad (18)$$

instead of (1), is solved first, considering  $v_0$  as the input. The solution of this problem,  $E_0, H_0, J_0, D_0$ , permits to determine the component  $i_0$  and the dynamic material characteristics given by:

$$\mu_d = \left. \frac{d\hat{B}}{dH} \right|_{H_0}, \quad \sigma_d = \left. \frac{d\hat{J}}{dE} \right|_{E_0}.$$

Then, the dynamic linear problem (1)-(3), (6)-(9) with

$$\vec{B} = \mu_d \vec{H}, \quad \vec{J} = \sigma_d \vec{E} \quad (19)$$

is solved, considering  $v^*$  as the input. The solution of this problem determine the component  $i^*$ .

The main disadvantage of this technique consist in the existence of two circuits, one for the quasi-static components  $v_0, i_0$  and other for the small signal components  $v^*, i^*$ . This disadvantage is eliminated in the large signal technique without a growth of the approximate error.

In the large signal technique the quasi-static problem (18), (2)-(9) under the input  $v$  is solved first, obtaining the fields  $E_0, H_0, J_0, D_0$ , under the eddy-current neglecting assumption.

Then, the nonlinear dynamic problem (1)-(3), (6)-(9) is solved, considering the material relations given by:

$$\vec{B} = \mu_d(\vec{H} - \vec{H}_0) + \vec{B}_0, \quad \vec{J} = \sigma_d(\vec{E} - \vec{E}_0) + \vec{J}_0. \quad (20)$$

The solution determines an approximate of the output  $i$ .

If the relations (4), (5) are linear, then the large signal equivalent circuit coincides with the small signal dynamic circuit, both being equivalent to the electromagnetic circuit element  $D_\Sigma$ .

If the material relations of  $D_\Sigma$  are nonlinear, then it is necessary that

$$|\hat{B}(\vec{H}) - \mu_d(\vec{H} - \vec{H}_0) - \vec{B}_0| \leq \epsilon \quad (21)$$

in order to limit the approximate error.

The inequality (21) is satisfied in the weak saturated ferromagnetic materials or for sufficiently slow time-varying fields.

### 2.3. Dipolar magnetic circuit element

A conducting cylinder of length  $L$  and of arbitrary shape cross-section  $S$ , with area  $A$ , having the electrical conductivity and nonlinear  $B/H$  relationship  $B = \hat{B}(H)$  is considered (Fig. 2). The magnetic field is consi-

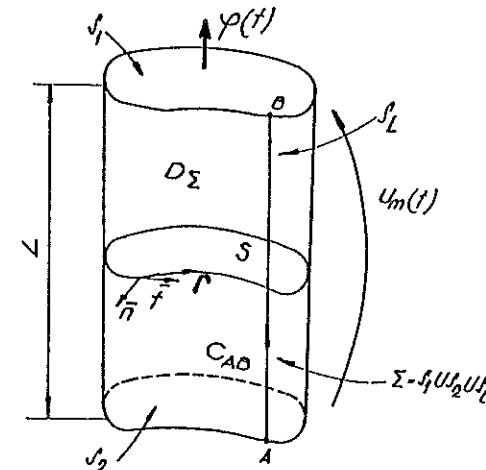


Fig. 2. The dipolar magnetic circuit element

dered two-dimensional  $\vec{H} = \vec{k} H(x, y, t)$ . Under these assumptions the conditions (6)-(9) involve the constancy of the magnetic field strength on the lateral surface  $S_1$ . Therefore the domain  $D_\Sigma$  is a dipolar magnetic circuit

element with the magnetic terminals  $S_1, S_2$ , whose input variable is magnetomotive force:

$$u_m(t) = \int_{C_{AB}} \vec{H} d\vec{r} = H_g \cdot L$$

and whose output variable is the magnetic flux:

$$\varphi(t) = \int_S \vec{B} d\vec{A}$$

through any cross-section  $S$ .

The electromagnetic field problem has the equations

$$\text{curl } \vec{H} = \vec{J} \quad (22)$$

$$\text{curl } \vec{E} = - \frac{\partial \vec{B}}{\partial t} \quad (23)$$

$$\vec{J} = \sigma \vec{E} \quad (24)$$

$$\vec{B} = \hat{B}(\vec{H}) \quad (25)$$

with the initial condition:

$$B(M, 0) = 0, \quad M \in S \quad (26)$$

and the boundary condition:

$$\vec{H}(M, t) = \vec{k} \cdot \vec{H}_g(t), \quad M \in \Gamma, \quad t \geq 0. \quad (27)$$

For the dipolar magnetic circuit element, thus defined, is required the small and large signal equivalent circuits, which will be determined in what follows.

### 3. SMALL SIGNAL MAGNETIC CIRCUITS

The magnetomotive force of dipolar magnetic element  $D_L$  is separated as:

$$u_m(t) = U_{mo} + u_m^*(t) \quad (28)$$

with bounded  $u_m^*(t)$ :  $|u_m^*(t)| \leq M_u$  and the magnetic flux is written also:

$$\varphi(t) = \phi_0 + \varphi^*(t). \quad (29)$$

If  $M_u$  is sufficiently small, then the domain  $D_L$  can be characterized by two equivalent circuits those presented in Fig. 3.

The nonlinear equivalent circuit (Fig. 3a) is valid for the quasi-static quantities  $U_{mo}$  and

$$\phi_0 = A \hat{B}(U_{mo}/L)$$

the eddy-currents being neglected.

The linear equivalent circuit shown in Fig. 2b is valid for the dynamic quantities  $u_m^*(t)$ ,  $\varphi^*(t)$  and it is described in the following theorem.

**Theorem 1** The dipolar magnetic circuit element  $D_L$  has an equivalent small signal circuit  $R, L$  which is parallel Foster's type with the parameters:

$$R_{pk} = \frac{L}{\mu_d b_k^2}, \quad L_{pk} = \frac{L}{\lambda_k b_k^2}, \quad k=1, 2, \dots \quad (30)$$

where  $\mu_d = \frac{d\hat{B}}{dH} \Big|_{H=U_{mo}/L}$ ,  $\lambda_k$  are the eigen values corresponding to normalized eigen functions  $\Psi_k$  of the operator  $-\Delta = -\frac{\partial^2}{\partial x^2} - \frac{\partial^2}{\partial y^2}$  under homogeneous Dirichlet boundary conditions and  $b_k$  is given by:

$$b_k = \int_S \Psi_k dA.$$

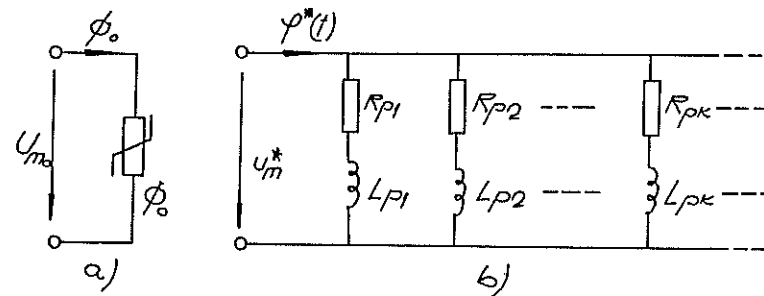


Fig. 3 The small signal equivalent circuits

**Proof** In the small signal technique, the problem (22)-(27) becomes:

$$\mu_d \sigma \frac{\partial \vec{H}}{\partial t} = \Delta \vec{H} \quad (31)$$

with the initial and the boundary conditions given by:

$$\vec{H}(M, t) = 0, \quad M \in S, \quad t = 0 \quad (32)$$

$$\vec{H}(M, t) = u_m/L = H_g, \quad M \in \Gamma, \quad t \geq 0. \quad (33)$$

Because  $S$  is a bounded surface, the eigen values problem:

$$-\Delta \Psi = \lambda \Psi, \quad \Psi|_{\Gamma} = 0$$

has a countable set of solutions and the eigen functions  $\Psi_k$  form an orthogonal, complete system. Therefore the solutions of the problem (31)-(33) can be written as:

$$\vec{H}(M, t) = H_g(t) + \sum_{k=1}^{\infty} a_k(t) \cdot \Psi_k(M) \quad (34)$$

whose  $a_k(t)$  coefficients satisfy the equations:

$$a'_k(t) = -\frac{\lambda}{\sigma \mu_d} a_k(t) - b_k H'_B(t). \quad (35)$$

The small signal magnetic flux is

$$\varphi(t) = \int_S \mu_d H dA = - \sum_{k=1}^{\infty} \frac{b_k \lambda_k}{\sigma} \int_0^t a_k dt = \sum_{k=1}^{\infty} \varphi_k.$$

Using (35), for each  $\varphi_k$ , we have:

$$\frac{d\varphi_k}{dt} = -\frac{\lambda_k}{\sigma \mu_d} \varphi_k + \frac{b_k^2 \lambda_k}{\sigma L} u_m(t) \quad (37)$$

which does represent an equation of the series R,L circuit. The identification permits to obtain the parameters (30).

#### 4. LARGE SIGNAL MAGNETIC CIRCUITS

Let consider the dipolar magnetic circuit element  $D_x$  and let suppose that the inequality (21) is satisfied with  $\epsilon$  sufficiently small. Applying the large signal technique, the equivalent circuit shown in Fig.4 is obtained, whose parameters are

$$L_{pk} = \frac{L \sigma \mu_d}{\lambda_k b_k^2 \mu_s}, \quad R_{pk} = \frac{L}{b_k^2 \mu_s}, \quad k=1,2,\dots \quad (38)$$

$$\text{where } \mu_d = \left. \frac{dB}{dH} \right|_{H=u_m/L}, \quad \mu_s = \left. \frac{dB}{dH} \right|_{H=u_m/L}.$$

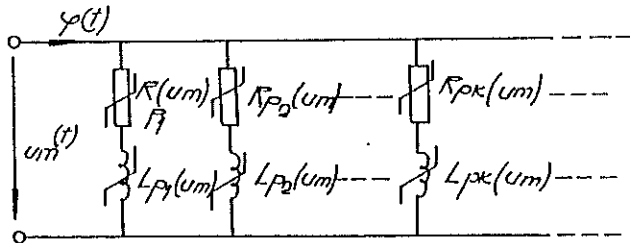


Fig.4 Large signal equivalent circuit

The following theorem allows to distinguish a general method for the large signal equivalent circuit construction.

**Theorem 2** If all the parameters  $R_k, L_k$  of the small signal linear equivalent circuit corresponding to the dipolar magnetic circuit element  $D_x$  are multiplied by

$\alpha(t) = \mu_d(t)/\mu_s(t)$  (where  $\mu_d$  and  $\mu_s$  are the dynamical and static permeabilities corresponding to the boundary field  $H_B = u_m(t)/L$ ), then the modified circuit is also as large signal equivalent circuit for the same domain  $D_x$ .

**Proof** In the large signal technique, the problem (22)-(27) becomes:

$$\int_0^t \Delta H dt = \sigma B$$

$$H(M,t) = u_m(t)/L = H_B(t), \quad M \in \Gamma \quad (39)$$

where  $B = \hat{B}(H) = B_B + \mu_d(H - H_B)$ . The solution of this problem can be expanded in a eigen function series

$$H(M,t) = H_B(t) + \sum_{k=1}^{\infty} a_k(t) \Psi_k(M) \quad (40)$$

where the coefficients  $a_k$  satisfy:

$$\lambda_k \int_0^t a_k(t) dt + \sigma \mu_d a_k(t) + \sigma b_k \hat{B}(H_B) = 0$$

The magnetic flux through  $D_x$  is given by:

$$\varphi = \int_S B dA = - \sum_{k=1}^{\infty} \frac{\lambda_k b_k}{\sigma} \int_0^t a_k(t) dt = \sum_{k=1}^{\infty} \varphi_k \quad (42)$$

Each of  $\varphi_k$  is the solution of differential equation:

$$\frac{d\varphi_k}{dt} = -\frac{\lambda_k}{\mu_d \sigma} \varphi_k + \frac{\lambda_k b_k^2 \mu_s}{\sigma \mu_d} \frac{u_m(t)}{L}. \quad (43)$$

The equation (43) allows to determine the relations (38), identifying it with a series R,L circuit equation.

It is simply to observe that the relations (38) can be obtained, multiplying the relations (30) by  $\mu_d/\mu_s$ .

Therefore the following lemma allows to finish this proof.

**Lemma 1.** The transformation of a linear passive dipolar R,L circuit by multiplying all parameters with the same function  $\alpha(t)$  has the property to preserve equivalence classes in the input-output meaning.

The state variables equations are used to prove this lemma.

In conclusion, the dipolar magnetic circuit element has a large signal magnetic equivalent circuit containing magnetic reluctances  $R_k$  and magnetic inductances  $L_k$  (for eddy-currents modeling) defined by the relations:

$$u_{mk}(t) = R_k(u_m) \cdot \varphi_k(t), \quad u_{mk}(t) = L_k \frac{d\varphi_k}{dt} \quad (44)$$

Therefore the equivalent circuit has nonlinear input-controlled parameters  $L(u_m), R(u_m)$ . For all that, if the input variable  $u_m(t)$  is known, then the equivalent circuit is a linear parametric one.

## 5. EQUIVALENT CIRCUITS OF COLS WITH SOLID CORES

Let consider a coil constructing of  $n$ -turns wound on the dipolar magnetic circuit element  $D_x$ , as a solid core. The cross-section area of the nonmagnetic media between the magnetic core and the winding is denoted by  $A_e$ .

The electric equivalent circuit of this coil is to determine.

Applying the electromagnetic induction law it results:

$$u_f - u = -L_e \frac{di}{dt} - n \frac{d\varphi}{dt} \quad (45)$$

where:  $u_f$  is the electrical tension along the coil wire,  $u$  is the terminal voltage of the coil,  $i$  is the coil current,  $\varphi$  is the core flux and

$$L_e = \frac{\mu_0 A_e}{L} n^2$$

is the leakage inductance.

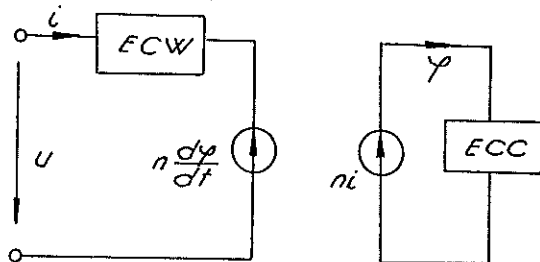


Fig.5 Equivalent network of coil

The relation (45) allows to synthesize an equivalent network (Fig.5) which is built by a magnetic and an electric circuits. The linkage between these circuits is made by using commanded sources. The dipole ECW denotes the equivalent circuit for the internal domain of wire (d.c. resistance  $r$  if the skin-effect is neglected) and ECC denotes the magnetic equivalent circuit for the core domain. This kind of network with commanded sources has the advantage to offer the

possibility of intricate devices analysis, e.g. the three-phase transformers transient analysis.

The following theorem allows to obtain an electric equivalent  $R, L$  circuit and to distinguish the duality between the electric equivalent circuits of coil and the magnetic equivalent circuits of core.

**Theorem 3** If the core domain  $D_x$  has planar-graph equivalent circuit with magnetic reluctances  $R_{mk}$  and magnetic inductances  $L_{mk}$ , then a large signal equivalent circuit of the coil wound on  $D_x$  can be obtained by applying the following procedure.

a. The circuit with the dual graph is constructed.

b. The magnetic reluctances  $R_{mk}$  are replaced by inductances  $L_k = n^2 / R_{mk}$ .

c. The magnetic inductances  $L_{mk}$  are replaced by resistances  $R_k = n^2 / L_{mk}$ .

d. To the circuit obtained as above the leakage inductance  $L_e$  and the dipolar equivalent circuit of the internal wire domain are serially connected.

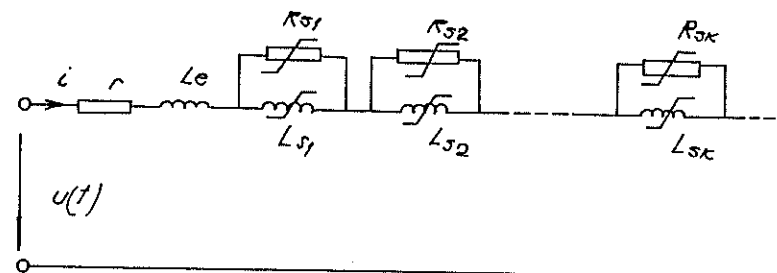


Fig.6 Equivalent circuit of coil

Applying this theorem is obtained the equivalent circuit shown in Fig.6. The circuit parameters are given by:

$$R_{sk} = \frac{n^2 \lambda_k b_k^2 \mu_B}{\sigma L \mu_d}, \quad L_{sk} = \frac{n^2 b_k \mu_B}{L} \quad k=1, 2, \dots \quad (46)$$

**Proof** According to (45) the terminal voltage is:

$$u(t) = r \cdot i(t) + L_e \frac{di}{dt} + \sum_{k=1}^{\infty} u_k \quad (47)$$

where  $u_k = n \frac{d\varphi_k}{dt}$ . Taking into account eqn. (44) and the equality  $u_m(t) = n i$  it results:

$$u_k(t) = - \frac{\lambda_k}{\sigma \mu_d} \int_0^t u_k(t) dt + n^2 \frac{\lambda_k b_k^2}{\sigma \mu_d} i. \quad (48)$$

Identifying the relation (48) with the parallel  $R_{sk}$ ,

$L_{sk}$  circuit equation, we obtain the relations (46).

Observing that the transformation which is introduced by procedure from theorem 3, has the property to preserve equivalence classes, this theorem has been proved

## 6. APPLICATIONS

Considering the dipolar magnetic element as a circular cylinder, it results the following eigen values  $\lambda_k$  and values of integrals  $b_k$ :

$$\lambda_k = \frac{z_k^2}{a^2}, \quad b_k = \frac{2a\sqrt{\pi}}{z_k} \quad (49)$$

where  $a$  is the radius of the cylinder and  $z_k$  are the roots of the Bessel's function  $J_0(z_k) = 0$ .

## 7. ACKNOWLEDGEMENTS

The author are indebted to the following Electrical Engineering Department of Politechnical Institut Bucharest staff: Prof. dr. C. I. Mocanu, Head of "Electrotehnic" Division for his encouragement throughout the work.

## 8. REFERENCES

1. Stoll, R L. The solution of transient and steady-state magnetic fields with particular reference to numerical methods. Proc. COMPUMAG, Oxford, 1976.
2. Silvester, P. Modal network theory of skin effect in flat conductors. Proc. IEEE, 54, 9, 1966.
3. Mocanu, C I. Equivalent schemes of the circular conductors at transient state with skin effect. Rev. Roum. Sci. Tech. 16, 2, 1971.
4. Kesavamurthy, N, Rajagopalan, P K. Effects of eddy currents on the rise and decay of flux in solid amagnetic cores. Proc. IEE 109C, 1962.
5. Silvester, P. Eddy current modes in linear solid-iron bars. Proc. IEE, 112, 8, 1965.
6. Mocanu, C I. Equivalent PSL schemes of coils with transient eddy current losses. Rev. Roum. Sci. Tech. 16, 3, 1971.
7. Ekelöf, S. Generalized reluctances in eddy current magnetic circuits. Arch. Electr. 49, 1, 1964.

8. Laithwaite, E R. Magnetic equivalent circuit for electrical machines. Proc. IEE, 114, 11, 1967.
9. Mocanu, C I. Linear magnetic circuits with eddy current losses in transient state. (in roum.), "Studii și cercetări de electrotehnică și energetică", 23, 1, Bucharest, 1973.
10. Subba Rao, V. Equivalent circuit of solid iron core for impact excitation problems. Proc. IEE, 111, 2, 1964.
11. Timotin, Al. Passive electromagnetic circuit element. (in roum.), "Stud. și cerc. de electr. și energ.", 21, 1, 1971.
12. Ioan, D C. Transient electromagnetic field in nonlinear media. Thesis, I.P. Bucharest, 1978.

# CONVERGENT ALGORITHM FOR UNBOUNDED, TWO-DIMENSIONAL, LINEAR EDDY CURRENT PROBLEMS

Charles W. Steele

Ampex Corporation, 401 Broadway, Redwood City, CA 94063

## ABSTRACT

This paper presents an iterative algorithm for computing a steady-state magnetic field with eddy currents in an unbounded region in which the medium is non-uniform in both conductivity and permeability. An analysis is presented that shows that circumstances under which convergence of this algorithm is assured. A computer program that uses this algorithm was written, and certain of its computed results are shown.

## INTRODUCTION

This paper is concerned with the problem of computing fields in an unbounded region, in the geometry shown in Fig. 1. In this geometry we have only the current carrying conductors and a magnetic core surrounded by free space.

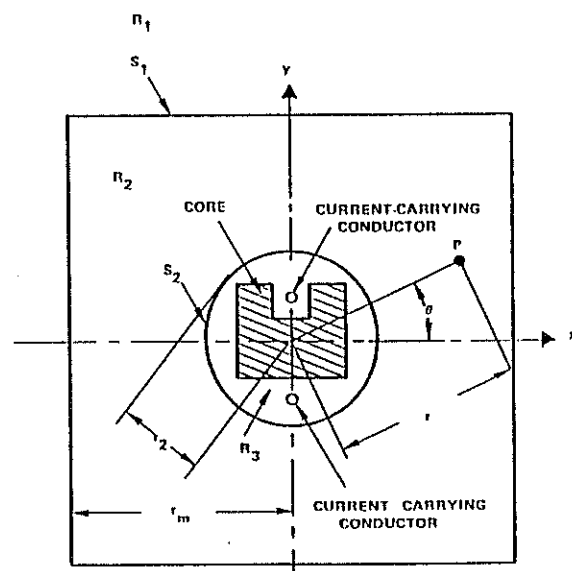


Fig. 1 Two-Dimensional Configuration

There are straightforward ways to compute fields numerically in a bounded region that contains a non-uniform medium, as well as ways to compute fields in an unbounded region that has a uniform medium. However, neither of the approaches is applicable by itself to the problem at hand, which combines a non-uniform medium with an unbounded region. It is, as a result, a difficult problem. This problem warrants considerable effort, however, since it arises quite often in science and engineering.

Roughly, one can categorize the methods used on this problem as "simultaneous" and "iterative". In a simultaneous method, correct and final field values are computed simultaneously at all points of interest in the region. Several papers<sup>1,2,3</sup> have reported simultaneous methods based upon using integral equations. In these algorithms, the non-uniformities in the medium are represented by equivalent source distributions that have the same effect upon the fields. Other papers<sup>4,5</sup> use the finite element method and handle non-uniformities by placing element boundaries along lines of discontinuity.

In an iterative method, one arbitrarily establishes a boundary (such as surface  $S_1$ , Fig. 1). All medium non-uniformities and all generators are contained within this boundary; outside this boundary there is only free space. The iterative method in general starts by putting approximate field values on an arbitrary boundary,  $S_1$ . Then the following sequence of steps is taken repeatedly:

- (1) Compute the fields inside  $S_1$ , as one would in any bounded region problem.
- (2) Using the results of Step (1), compute new field values on  $S_1$ .

Sandy and Sage,<sup>6</sup> and Cermak and Sylvester<sup>7</sup>, have reported the development and use of iterative methods.

In this paper the development and use of another iterative method is reported. This method differs from the methods mentioned above by the algorithm used in Step (2). This method is applied to the computation of fields in and around a magnetic core that is permeable and conductive. Specifically the magnetic vector potential,  $A$ , is computed throughout the Fig. 1 configuration. It is proven that this method converges to the right answer from any starting values. Finally, test results are shown and discussed.

## CONFIGURATION AND FIELDS

The configuration, shown in Fig. 1 consists of a magnetic core and two conductors, surrounded by free space. The conductors carry currents equal in magnitude and opposite in direction. The core is highly permeable and conductive, and the permeability and conductivity are uniform inside it. This is a two-dimensional configuration in which there are no variations in the  $z$  direction (into the paper).  $A$  and  $J$ , (the magnetic vector potential and the current density) have only  $z$

components, and  $H$ , the magnetic field, has only  $x$  and  $y$  components. By physical reasoning, these assumptions can be shown to apply to this configuration.

Over the current carrying conductors,

$$\nabla^2 A_z = -\mu J_g \quad (1)$$

where  $J_g$  is the current density in the conductors. Inside the core material,

$$\nabla^2 A_z = j \omega \mu \sigma A_z \quad (2)$$

where  $\mu$  and  $\sigma$  are the permeability and conductivity, and in the free-space portion of the configuration,

$$\nabla^2 A_z = 0 \quad (3)$$

All of space is divided into Regions  $R_1$ ,  $R_2$  and  $R_3$ .  $R_1$  and  $R_2$  are separated by surface  $S_1$ , and  $R_2$  and  $R_3$  are separated by surface  $S_2$ . Surface  $S_2$  is a circular cylinder of radius  $R_2$  whose axis passes through the origin.

#### ALGORITHM

The first step of the algorithm is to place approximate values of the computed field,  $A_{zc}$ , on  $S_1$ . Following this, a number  $M$ , of computation cycles are taken, each cycle consisting of the following steps:

(a) Compute  $A_{zc}$  throughout  $R_2$  and  $R_3$ .

This is done so as to satisfy Equations (1), (2), and (3) to make  $A_{zc}$  continuous across the core surfaces and to match whatever boundary values have been most recently placed on  $S_1$ . A successive over-relaxation method is used over a square grid of points. The finite difference formulation used is essentially that given by Stolt<sup>8</sup>. This step comprises a certain number,  $N$ , of sweeps and each sweep covers  $R_2$  and  $R_3$ .

(b) From the results of (a), find  $A_{zc}$  on  $S_2$ .

(c) From the results of (b), compute  $A_{zc}$  throughout  $R_1$  and  $R_2$ .

Note that  $R_1$  and  $R_2$  comprise all of space outside  $S_2$ . Thus, the exterior solution of Equation (3) in cylindrical coordinates holds, namely,\*

$$A_{zc} = \sum_{i=1}^n C_i \sin(i\theta + \alpha_i) r^{-i} \quad r \geq r_2 \quad (4)$$

where  $n$  is some large integer. From Equation (4) and the results of (b), we can compute  $C_i$  for

$$1 < i \leq n$$

(d) Using (4), compute new values of  $A_{zc}$  on  $S_1$ .

The algorithm comprises an inner loop and the outer loop. The inner loop is contained within Step (a). Its cycle is a successive over-relaxation sweep across  $R_2$  and  $R_3$ , which is executed  $N$  times. A cycle of the outer loop comprises Steps a, b, c and d; and this cycle is executed  $M$  times. No provisions were built into the computer program for terminating either the inner loop or the outer loop automatically, since there are no simple and adequate criteria for these terminations. The values of  $M$  and  $N$  were input to the computer at the beginning of each run.

#### CONVERGENCE PROOF

##### A. Error Field

For the proof, the computed field,  $A_{zc}$  is separated into two components,  $A_{za}$ , the actual, correct field, and  $A_{ze}$ , the error field so that

$$A_{ze} = A_{zc} - A_{za} \quad (5)$$

Equations (6) through (9) below give expressions for  $\nabla^2 A_{zc}$  and  $\nabla^2 A_{za}$  over the current-carrying conductors, over the core material and throughout free space. In these equations, the expressions for  $\nabla^2 A_{za}$  are dictated by the physics of the problem. On the other hand, the expressions for  $\nabla^2 A_{zc}$  are prescribed by the algorithm.

\*Note that the net current inside  $S_2$  in the  $z$  direction is zero. From this fact, one can show that the term  $\log r$  (which is a part of the general exterior solution of Equation (3) cylindrical coordinates) cannot be present in Equation (4).

Over the current-carrying conductor, we have

$$\nabla^2 A_{za} = \nabla^2 A_{zc} = -\mu J_g \quad (6)$$

Throughout  $R_1$ ,  $R_2$  and the free-space part of  $R_3$ , we have

$$\nabla^2 A_{za} = \nabla^2 A_{zc} = 0 \quad (7)$$

Within the core material, we have

$$\nabla^2 A_{za} = j\omega\mu\sigma A_{za} \quad (8)$$

$$\nabla^2 A_{zc} = j\omega\mu\sigma A_{zc} \quad (9)$$

From (5) through (9), we see that

$$\nabla^2 A_{ze} = j\omega\mu\sigma A_{ze} \quad (10)$$

over the magnetic core and that

$$\nabla^2 A_{ze} = 0 \quad (11)$$

over the current carrying conductor and over free space.

As required in the proof below, an equation is now derived for the Laplacian of  $|A_{ze}|^2$ , that applies to every point in this configuration except on the core-to-free-space interface. (This Laplacian cannot be defined on that interface.) By vector analysis identities we have

$$\nabla^2 |A_{ze}|^2 = A_{ze} \nabla^2 \bar{A}_{ze} + \bar{A}_{ze} \nabla^2 A_{ze} + 2 |\nabla A_{ze}|^2 \quad (12)$$

where  $\bar{A}_{ze}$  denotes the complex conjugate of  $A_{ze}$ . At any point at which either Equation (10) or Equation (11) holds, Equation (12) becomes

$$\nabla^2 |A_{ze}|^2 = 2 |\nabla A_{ze}|^2 \geq 0 \quad (13)$$

Thus, Inequality (13) holds at every point in Fig. 1 except points on the core-to-free-space interface.

## B. Error Field at End of Step (a) of Algorithm

We proceed to show that at the end of Step (a) of the algorithm, the values of  $|A_{ze}|$  at points inside  $S_1$  are less than the maximum of  $|A_{ze}|$  on  $S_1$ .

First, we deal separately with points on the core-free-space interface, since Inequality (13) does not apply to the interface. By contradiction, suppose that there were a maximum of  $|A_{ze}|$  and  $|A_{ze}|^2$ , on the interface at point P, as shown in Fig. 2. Then there would have to be a closed path C, surrounding P, over which the vector outflow of

$$\mathbf{V} = \frac{1}{\mu} \nabla |A_{ze}|^2$$

is negative. But by Inequality (13), and the divergence theorem, this vector outflow is non-negative. Thus,  $|A_{ze}|$  cannot have a maximum at P.

Inequality (13) precludes the possibility of a local maximum occurring inside  $S_1$ , at points not on the interface. Thus, at no point inside  $S_1$  can  $|A_{ze}|$  exceed the maximum on  $S_1$ . Since that would require a global maximum (which is also a local maximum) inside  $S_1$ . Further, at no points inside  $S_1$  can  $|A_{ze}|$  equal its maximum on  $S_1$ , if those points would form local maxima. Thus, the only way that  $|A_{ze}|$  at points inside  $S_1$  could equal the maximum on  $S_1$  would be if a maximum contained both points on  $S_1$  and adjacent points inside  $S_1$ . But again, we can use Inequality (13) to show that such a maximum is not possible.

Therefore, the values of  $|A_{ze}|$  at all points inside  $S_1$  at the end of Step (a) are less than the maximum on  $S_1$ .

## C. Error Field at End of Step (c) of Algorithm

We proceed to show that the error field at the end of Step (c) of the algorithm is less outside  $S_2$  than its maximum on  $S_2$ . Let  $r$  be the distance from any point outside  $S_2$  to the center of circle  $S_2$ . Since we know that

$$\lim_{r \rightarrow \infty} |A_{ze}| = 0$$

then there is a number,  $c$  such that if  $r > c$  then  $|A_{ze}|$  is less than its maximum value on  $S_2$ .

Then we have an annulus that is bounded by  $S_2$  on the inside and a circle of radius  $c$  on the outside. We need only show that  $|A_{ze}|$  at all points within this annulus is less than its maximum value in  $S_2$ . That proof follows along the lines given above.



#### D. Convergence

Part B above shows that field values on  $S_2$  at the end of Step (b) of the algorithm have a smaller maximum error than the maximum error on  $S_1$  during the preceding Step (a). Part C shows that field values on  $S_1$  computed by Step (d) of the algorithm have a smaller maximum error than the maximum error on  $S_2$  at the end of the preceding Step (b). Thus, the algorithm converges to the right answer provided that  $S_1$  is totally outside  $S_2$ .

#### E. Application of Convergence Proof to the Computer Program

The algorithm that is used to compute the results shown in the next section differs somewhat from the algorithm presumed for the convergence proof above. For one thing, the convergence proof presumes that fields are computed at all points on  $S_1$ ,  $S_2$ , and over  $R_2$  and  $R_3$ , while the computer program, of course, computes the field over a finite number of points, distributed over these surfaces and regions. This is an insignificant difference, however, since, in practice, we choose our spacing between points to be small enough that the discretization error is within acceptable bounds.

A more significant difference relates to the computation of field throughout  $R_2$  and  $R_3$  in Step (a). The convergence proof presumes that this computation is exact, subject to the boundary conditions on  $S_1$ . In this computer program, this is an iterative computation and is therefore not exact.

The accuracy depends upon  $N$ , the number of sweeps used. If  $N$  is too small, we can find that the algorithm either converges slowly or not at all. If  $N$  is too large, we can be wasting computer time. A value of  $N = 10$  was found to be about optimum.

#### COMPUTED RESULTS

The author wrote and tested a computer program that uses the algorithm described above. Early in these tests, the algorithm was found to converge to the correct boundary conditions on  $S_1$ , much more rapidly using a coarse mesh of computation points than using a fine mesh. For this reason, the program was refined to include the following stages:

Stage 1 - Compute the field using a coarse grid until convergence is achieved in terms of the field, both on  $S_1$  and inside  $S_1$ .

Stage 2 - By interpolation, create a finer grid that covers the same area but uses a point-to-point spacing that is half the previous value.

Stage 3 - Again compute the field using the fine grid until convergence is achieved.

This computer program was tested for two configurations. The first of these configurations comprises the two current-carrying conductors in Fig. 1 but without the magnetic core. This configuration was chosen because its field can be computed analytically, and this provides a means for testing the accuracy of the algorithm. Although badly erroneous starting values were used on  $S_1$  (intentionally) the program converged quickly and smoothly to the correct field values.

The second configuration is just that of Fig. 1. Figs. 3, 4 and 5 show contour plots of  $|A_z|$  (at levels chosen by the fourth power) for one half of the Fig. 1 configuration. Fig. 3 is plotted before the algorithm is used and Fig. 4 is plotted after it has been executed 40 times. The arrows on these figures point to the same level of  $|A_z|$  and illustrate how much the boundary values on  $S$  have changed. Fig. 5 is a close-up of the core at the end of the computation, after the algorithm has been executed 20 more times.

#### REFERENCES

1. Fawzi and Burke, "Use of Surface Integral Equations for Analysis of TM-Induction Problem", Proc. IEE, Vol. 121, No. 10, October, 1974.
2. C. Steele and J. Mallinson, "Theory of Low Permeability Heads", 1972 INTERMAG Conference, IEEE Transactions on Magnetics, September, 1972, Vol. MAG-8, pp. 503-505.
3. G. Jeng and A. Wexler, "Isoparametric, Finite Element, Variational Solution of Integral Equations for Three-Dimensional Fields", International Journal for Numerical Methods in Engineering, Vol. 11, 1977, pp. 1455-1471.
4. B. McDonald and A. Wexler, "Finite-Element Solution of Unbounded Field Problems", IEEE Transactions on Microwave Theory and Techniques, Volume MTT-20, Number 12, December, 1972, pp. 841-847.
5. P. Silvester, D. Lowther, C. Carpenter, E. Wyatt, "Exterior Finite Elements for 2-Dimensional Field Problem with Open Boundaries", Proc. IEEE, Vol. 124, No. 12, December, 1977.

6. Sandy and Sage, "Use of Finite Difference Approximations to Partial Differential Equations for Problems Having Boundaries at Infinity", IEEE Transactions on Microwave Theory and Techniques, May 1971, pages 484-486.
7. I. Cermak and P. Silvester, "Solution of 2-Dimensional Field Problems by Boundary Relaxation", Proc. IEE, Vol. 115, No. 9, September, 1968, pp. 1341-1348.
8. Richard L. Stoll, "The Analysis of Eddy Current", Clarendon Press, Oxford, 1974.

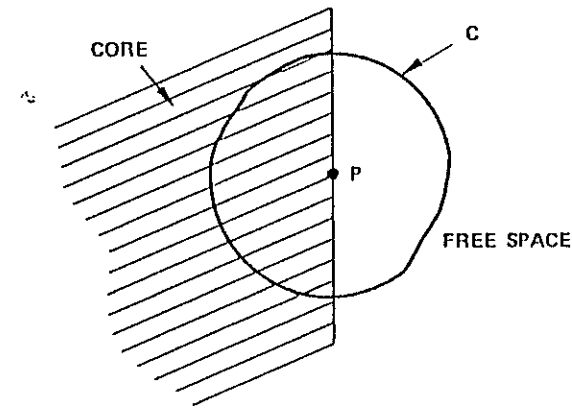


Figure 2 Point on Core Surface

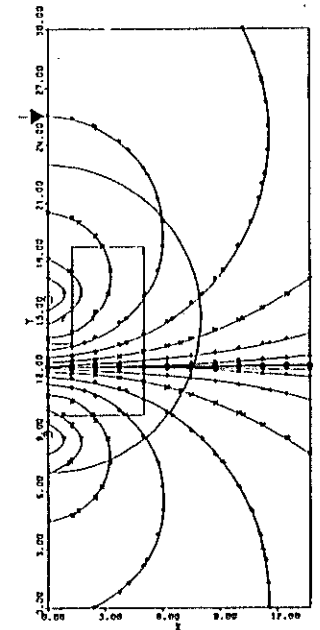


Figure 3 Field at Start of Computation

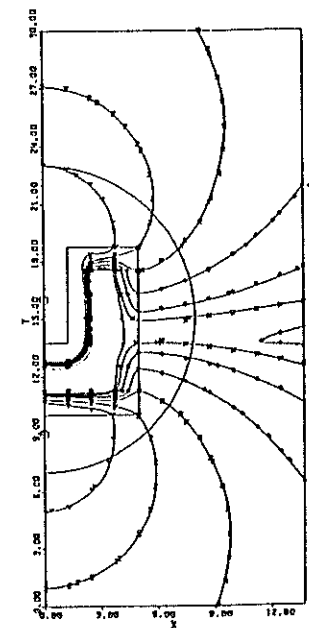


Figure 4 Field After Computation

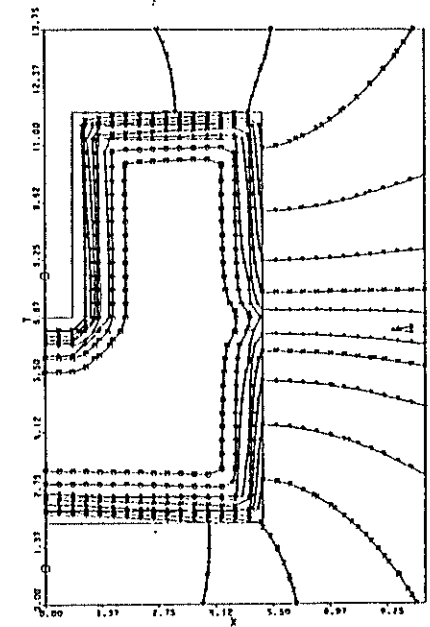


Figure 5 Close-up of Field After More Computation

## GENERAL DISCRETE EQUATIONS FOR LAMINATED CORES

T.G. Phemister

N.E.I. Parsons Ltd, Newcastle upon Tyne, NE6 2YL, England

## ABSTRACT

To investigate the effect of gaps between laminations on axial flux and eddy currents near the end of a stator core, general discrete equations have been developed. The equations are obtained by integrating Maxwell's equations across the thickness of a lamination and then simplified by the assumption that the mean value of each component of the magnetic field across a lamination is equal to the average of its values on either side. In their simplified form, the equations are well suited to solution by an iterative method.

## 1. INTRODUCTION

There is one simplification which is forced on anyone who seeks to calculate the three-dimensional electromagnetic fields in a generator stator: a smoothed or homogeneous<sup>1</sup> representation of the laminar structure must be used. The number of layers of laminations in the first half metre from the end is of the order of a thousand, and the number of individual laminations of the order of ten thousand; it is not possible to model each separately. However, the gaps between laminations must change the pattern of the eddy currents in comparison with a similar core which had no such electrical discontinuities in the circumferential direction. Work on the effect of the gaps in an idealised core<sup>2</sup> showed it to be significant, changing the axial flux by 20% and the total eddy current loss by more than 30%; that suggested the need to investigate the effect of the gaps near the core end, where the idealised model was inappropriate.

Near the end of the stator core, the circumferential component of eddy current is more widely spread over the radial width of the core than it is further in, where the phenomenon of skin-depth concentrates it near the teeth and slots and near the outer surface. The effect of gaps between laminations will, therefore, be greater near the end of the core, because the gaps can inhibit widely spread currents more than constricted currents. Since the effect is already

of order 20% further in, it will certainly be significant at the end. Work has been undertaken to quantify it, with the aim of correcting the larger-scale three-dimensional calculations, based on a smoothed model of the core, to allow for discrete effects of separate laminations near the core end. The scope of the present paper is more limited. It will be shown how an assumption which is unlikely to cause significant error permits the development of a convenient set of equations, and a method of solving them will be indicated.

## 2. GENERAL ASSUMPTIONS

The following general assumptions are made: that only power frequencies are of interest and that the displacement current can be neglected; that the material of the core-plate is perfectly uniform (though not necessarily isotropic) in its properties, its micro-structure being neglected; that the faces of the laminations are all perfectly parallel and perpendicular to the axis of the machine; that the electrical resistivity of the core-plate material is constant throughout each lamination.

## 3. PRELIMINARY NOTATION

The following notation will be used in the development of the equations and is intended to make the algebra easy to follow. Some of it will, however, be abandoned later, to simplify the equations.

Cartesian coordinates  $x$ ,  $y$ ,  $z$  will be used, the directions of the  $x$  and  $y$  axes being parallel to the laminations, and the direction of the  $z$  axis perpendicular to them.  $x$ ,  $y$  and  $z$  will be used as suffices to denote the components of vectors.

The usual notation of  $\underline{B}$ ,  $\underline{H}$  and  $\underline{J}$  for the vectors of flux density, magnetising force, and current density will be employed.

Similarly,  $\rho$  and  $\mu_0$  will be used for the resistivity of the core-plate material and the fundamental constant of permeability.

The superfixes  $-$ ,  $+$ , and  $m$  will be used to denote the value of any quantity on either face of a lamination or its mean value across the lamination. Thus, for example,

$H_x^-$  is the value of  $H_x$  on the face of the lamination for which the coordinate  $z$  is lesser,

$H_x^+$  is the value of  $H_x$  on the face of the lamination for which the coordinate  $z$  is greater,

$H_x^m$  is the mean value of  $H_x$  across the lamination.

The width of the lamination is  $2a$ .

#### 4. EQUATIONS WITHIN A LAMINATION

Integrating the equation  $\text{div } \underline{J} = 0$  across the lamination gives

$$\frac{\partial J_x^m}{\partial x} + \frac{\partial J_y^m}{\partial y} = 0,$$

since  $J_z = 0$  on both faces of the lamination. Hence, a mean stream function,  $T$  say, exists, such that

$$J_x^m = \frac{\partial T}{\partial y} \quad \text{..... (1)}$$

$$\text{and } J_y^m = -\frac{\partial T}{\partial x}. \quad \text{..... (2)}$$

Integrating the  $x$  and  $y$  components of the equation  $\text{curl } \underline{H} = \underline{J}$  across the lamination gives

$$H_y^+ - H_y^- = 2a \left( \frac{\partial H_z^m}{\partial y} - J_x^m \right) \quad \text{..... (3)}$$

$$\text{and } H_x^+ - H_x^- = 2a \left( \frac{\partial H_z^m}{\partial x} + J_y^m \right). \quad \text{..... (4)}$$

Since  $J_z = 0$  on both faces of the lamination, it must be possible to derive both  $H_x^+$ ,  $H_y^+$  and  $H_x^-$ ,  $H_y^-$  from scalar potentials. Consequently a scalar potential,  $s$ , can be defined such that

$$\frac{1}{2}(H_x^+ - H_x^-) = -\frac{\partial s}{\partial x} \quad \text{..... (5)}$$

$$\text{and } \frac{1}{2}(H_y^+ - H_y^-) = -\frac{\partial s}{\partial y}. \quad \text{..... (6)}$$

If equations 1, 2, 5 and 6 are substituted in equations 3 and 4 and the latter equations are integrated, then

$$T = \frac{s}{a} + H_z^m + f(t), \quad \text{..... (7)}$$

where  $f(t)$  is a function of time only, but may take different values

for different laminations even in the same layer.

Integrating the equation  $\text{div } \underline{B} = 0$  across the lamination gives

$$2a \left( \frac{\partial B_x^m}{\partial x} + \frac{\partial B_y^m}{\partial y} \right) = - (B_z^+ - B_z^-). \quad \text{..... (8)}$$

Integrating the  $z$  component of the equation  $\rho \text{curl } \underline{J} = -\frac{\partial \underline{B}}{\partial t}$  across the lamination and substituting from equations 1 and 2 gives

$$\nabla^2 T = \frac{1}{\rho} \frac{\partial B_z^m}{\partial t}, \quad \text{..... (9)}$$

where  $\nabla^2$  is the two-dimensional Laplacian operator.

#### 5. A SIMPLIFICATION

Apart from the general assumptions of Section 2, no simplification has yet been made. However, the equations which link one lamination with another can contain only the values of the fields on the faces of the laminations, whereas Equations 7, 8 and 9 contain also average values of the fields across the laminations. There is little that can be done with the equations without introducing a simplification: that the mean value across the lamination of any component of  $\underline{H}$  or  $\underline{B}$  is equal to the average of its values on the two faces of the lamination, i.e.  $H_x^m = \frac{1}{2}(H_x^+ + H_x^-)$ , etc. This is the crucial simplification which makes possible the setting up of a convenient set of equations; its validity will be investigated in Section 9.

Since the laminations are thin, the simplification effectively implies that the variation in permeability across the lamination is negligible. Alternatively, this can be regarded as an independent simplification. It cannot be far from the truth because the constraint on the fields to minimise the magnetic energy would preclude significant variations in the degree of saturation across a thin lamination. This simplification implies that the permeability depends only on  $\underline{H}^m$  (and its history, if hysteresis is included in the calculations) or on  $\underline{B}^m$  (and its history).

## 6. FURTHER NOTATION

With the simplification of Section 5, it is possible to define a scalar potential,  $S$ , axial flux densities,  $B$  and  $b$ , and components of permeability,  $\mu_x$ ,  $\mu_y$ ,  $\mu_z$ , such that

$$\begin{aligned} H_x^m &= \frac{1}{2}(H_x^+ + H_x^-) = -\frac{\partial S}{\partial x}, \\ H_y^m &= \frac{1}{2}(H_y^+ + H_y^-) = -\frac{\partial S}{\partial y}, \\ B_z^m &= \frac{1}{2}(B_z^+ + B_z^-) = B, \\ \frac{1}{2}(B_z^+ - B_z^-) &= b, \\ (B_x^m, B_y^m, B_z^m) &= (\mu_x H_x^m, \mu_y H_y^m, \mu_z H_z^m). \end{aligned}$$

7. FINAL EQUATIONS WITHIN LAMINATIONS IN LAYER NO.  $n$ 

The notation of Section 6 will be employed to simplify Equations 7, 8 and 9. At the same time, in preparation for the equations which link laminations, the suffix  $n$  will be introduced, to indicate that the equations refer to the layer of laminations numbered  $n$ . Equations 7, 8 and 9 become:

$$T_n = \frac{1}{\alpha_n} s_n + \frac{1}{\mu_z} B_n + f_n(t), \quad \dots (10)$$

$$\frac{\partial}{\partial x} \left( \mu_x \frac{\partial S_n}{\partial x} \right) + \frac{\partial}{\partial y} \left( \mu_y \frac{\partial S_n}{\partial y} \right) = \frac{1}{\alpha_n} b_n, \quad \dots (11)$$

$$\nabla^2 T_n = \frac{1}{\alpha_n} \frac{\partial B_n}{\partial t}, \quad \dots (12)$$

Strictly,  $\mu_x$ ,  $\mu_y$ ,  $\mu_z$  should have been given the suffix  $n$ , but no confusion will arise from its omission.

$f_n(t)$  disappears if the right-hand side of Equation 10 is substituted for  $T_n$  in Equation 12. Any convenient value can therefore be assigned to it at each instant of time.

## 8. EQUATIONS BETWEEN LAMINATIONS

The non-magnetic, non-conducting region between adjacent layers of laminations is very thin, usually between 15 and 40  $\mu\text{m}$ , and it is disproportionately affected by any irregularities in the surface of the core-plate. Any refinement in the mathematical treatment of the magnetic field in such a region would be ridiculous; it will be assumed that the axial component of flux density does not vary across these regions, i.e.

$$B_n + b_n = B_{n+1} - b_{n+1}. \quad \dots (13)$$

With the same assumption, integration of the  $x$  and  $y$  components of  $\text{curl } \underline{H} = \underline{Q}$  gives

$$B_n + b_n = \frac{\mu_0}{h_n} (S_n + s_n - S_{n+1} + s_{n+1}) + g_n(t), \quad \dots (14)$$

where  $h_n$  is the width of the non-magnetic region between layer  $n$  and layer  $n+1$  of the laminations and  $g_n(t)$  is a function of time only.

There is a difficulty, however. If, as in Section 5, it had been assumed that the mean value of the field across the region between layers was equal to the average of its values on either side, Equation 14 would have been unchanged, but Equation 13 would have been replaced by

$$B_{n+1} - b_{n+1} - B_n - b_n = \frac{1}{2} \mu_0 h_n \nabla^2 (S_{n+1} - s_{n+1} + S_n + s_n), \quad \dots (15)$$

obtained by integrating  $\text{div } \underline{B} = 0$  across the region. The presence of the very small  $h_n$  in the numerator of the right-hand side of Equation 15, as compared with its position in the denominator in Equation 14, indicates that Equation 13 is a very good approximation indeed. At the same time, the omission of the right-hand side of Equation 15 means that some magnetic flux is unaccounted for, which is always unwise when calculations are required for ferromagnetic materials.

The flux unaccounted for is small and would not justify the complication of replacing Equation 13 by Equation 15, but there is a simple way of accommodating it without making the equations generally less tractable. If there are  $N$  layers of laminations in all, summing the right hand side of Equation 15 from 1 to  $N-1$  gives

$$\frac{1}{2} \mu_0 \nabla^2 \left[ h_1 (S_1 + s_1) + h_{N-1} (S_N - s_N) + \sum_{n=2}^{N-1} (h_n + h_{n-1}) S_n \right].$$

This suggests that there would be little error in making the divergence equation (11) cover half the non-magnetic region on either side of the core-plate, to give

$$\frac{\partial}{\partial x} [(a_n \mu_x + d_n \mu_o) \frac{\partial S_n}{\partial x}] + \frac{\partial}{\partial y} [(a_n \mu_y + d_n \mu_o) \frac{\partial S_n}{\partial y}] = b_n, \quad \dots (16)$$

where  $d_1 = \frac{1}{2} h_1$ ,

$$d_N = \frac{1}{2} h_{N-1},$$

$$d_n = \frac{1}{2} (h_{n-1} + h_n), \quad n = 2, N-1.$$

Replacing Equation 11 by Equation 16 means that the only flux unaccounted for in dropping the right-hand side of equation 15 is in the two terms with  $s_1$  and  $s_N$ . However,  $\nabla^2 s_n$  is much smaller than  $\nabla^2 S_n$  where the lamination is saturated and is negligible where the lamination is not saturated, and so the replacement of Equation 11 by Equation 16 is an accurate way of compensating the error in reducing Equation 15 to Equation 13. The greatest advantage in moving from Equation 11 to Equation 16 is that it allows the analysis to be applied to radial cooling ducts with little error.

## 9. ASSESSMENT OF SIMPLIFICATIONS

Apart from the general assumptions of Section 2, three simplifications have been made. The assumption that  $B_z$  does not vary across the non-magnetic region between laminations has been discussed in Section 8, where it was shown how the small error could be compensated elsewhere. The assumption that the permeability does not vary across the width of a lamination should cause negligible error. Only the remaining simplification, that the mean value of

the magnetic field across a lamination is equal to the average of its values on either side, requires further investigation.

If  $H_x^m$  and  $H_y^m$  differ from  $\frac{1}{2}(H_x^- + H_x^+)$  and  $\frac{1}{2}(H_y^- + H_y^+)$  significantly, then it must be because of eddy-currents; a one-dimensional linear analysis can quantify the possible error. If the relative permeability is  $\mu_r$ , a constant,  $\omega$  is the circular frequency, and  $\alpha = \alpha^2 \omega \mu_0 \mu_r / \rho$ , the relative error is

$$\frac{7\alpha^2}{90} + O(\alpha^4) \text{ in modulus, and } \frac{\alpha}{3} + O(\alpha^3) \text{ radians in phase.}$$

For 0.5mm core-plate at a frequency of 60 Hz, this means a relative error of approximately  $3 \times 10^{-10} \mu_r^2$  in modulus, and  $2 \times 10^{-5} \mu_r$  radians in phase.

These are extreme values, since the error in the solutions will be less than the error in the approximation. For completely unsaturated core-plate this can mean a relative error up to 20% in modulus and 30° in phase, but even slight saturation makes the error negligible. A relative permeability of 6000, for example, would imply a relative error less than 1% in modulus and 7° in phase.

The high relative error in the magnetising force in unsaturated regions is negligible for the solution as a whole, because the absolute value of the magnetising force is so small that the error does not matter. As so often in calculations of fields in ferromagnetic material, it is only in the saturated regions that it is necessary to calculate the magnetising force accurately, and in these regions the error of the simplification is very small. The  $x$  and  $y$  components of  $B$  do not enter the calculation directly.

The other part of the simplification, that  $B_z^m = \frac{1}{2}(B_z^+ + B_z^-)$ , can be investigated by supposing that

$$B_z = B_z^m + \left(\frac{z}{\alpha}\right) B_{z1} + \left(\frac{z}{\alpha}\right)^2 B_{z2},$$

$$B_x = B_x^m + \left(\frac{z}{\alpha}\right) B_{x1},$$

$$\text{and } B_y = B_y^m + \left(\frac{z}{\alpha}\right) B_{y1},$$

$z$  being measured from the centre of the lamination. Then the equation  $\text{div } \underline{B} = 0$  gives

$$\frac{\partial B_{x1}}{\partial x} + \frac{\partial B_{y1}}{\partial y} = -\frac{2}{a} B_{z2}.$$

Thus, in 0.5 mm core-plate the cumulative effect of  $B_{z2} = 10$  mT over a length of 6 mm would be to cause the huge difference of 1T between the two faces of the core-plate in the flux density parallel to the lamination.  $B_{z2}$  of any size can, therefore, exist only locally, and setting  $B_z^m = \frac{1}{2}(B_z^+ + B_z^-)$  can cause little error in the solution as a whole.

To sum up, the simplifications will produce a negligible error in the solution as a whole, though they may cause local errors in unsaturated regions.

#### 10. THE COMPLETE SET OF EQUATIONS

The equations will be rearranged and one of them will be eliminated. The first is Equation 13, the second comes from eliminating  $\sigma_n$  and  $\sigma_{n+1}$  between Equations 10 and 14, and the third and fourth are Equations 16 and 12, respectively.

$$b_n + b_{n+1} = B_{n+1} - B_n, \quad n = 1, N-1. \quad \dots (17)$$

$$a_n T_n + a_{n+1} T_{n+1} - \frac{h_n b_n}{\mu_0} = S_{n+1} - S_n + \left( \frac{h_n}{\mu_0} + \frac{a_n}{\mu_{zn}} \right) B_n + \frac{a_{n+1} B_{n+1}}{\mu_{z,n+1}}, \quad n = 1, N-1. \quad \dots (18)$$

$$\frac{\partial}{\partial x} \left( (a_n \mu_x + d_n \mu_0) \frac{\partial S_n}{\partial x} \right) + \frac{\partial}{\partial y} \left( (a_n \mu_y + d_n \mu_0) \frac{\partial S_n}{\partial y} \right) = b_n, \quad n = 1, N. \quad \dots (19)$$

$$\frac{\partial B_n}{\partial t} = \rho_n \nabla^2 T_n, \quad n = 1, N. \quad \dots (20)$$

$f_n(t)$  and  $g_n(t)$  have been set to zero.

This can always be done by adjusting the boundary conditions. In a heteropolar field,  $g_n(t)$  is necessarily zero.

#### 11. A METHOD OF SOLUTION

Equations 17 to 20 are well suited to an iterative method of solution. First, starting values of  $B_n$  and  $S_n$  are set up for each point in space and time. Then the following four steps are repeated until convergence is obtained.

1. Equations 17 and 18, supplemented by the two boundary conditions at the ends, are solved for  $b_n$  and  $T_n$  for each point in the  $x, y$  plane and each point of time.
2. Round the boundary of each lamination,  $T_n$  is set to a constant for each point in time.
3. A single Newton-Raphson step is taken in solving Equation 19 for  $S_n$  for each layer of laminations at each point in time.
4. Equation 20 is solved for  $B_n$  for each point in space.

This method of solution is similar to the way in which quasi-steady fields become established during transient conditions in an actual machine and instability should be easily avoided. Convergence should be quicker than by a straightforward relaxation since, during a single iterative cycle, all interior points are directly influenced by all the boundary conditions. Equations 17 and 18 bring in the boundary conditions at the axial ends, Equation 19 the boundary conditions at surfaces parallel to the axis, and Equation 20 the condition that the fields are periodic in time.

#### 12. CONCLUSION

A simplification which introduces little error permits the development of a convenient set of equations for the electromagnetic fields in laminated cores and makes possible the calculation of discrete effects of the laminar structure.

#### 13. ACKNOWLEDGEMENTS

The work formed part of a joint programme of research by N.E.I. Parsons Ltd. and the Central Electricity Generating Board. The author wishes to thank N.E.I. Parsons for permission to publish and Dr.D.A.H. Jacobs of the C.E.G.B. and Professor P. Hammond of Southampton University for their encouragement.

#### 14. REFERENCES

1. Jacobs, D.A.H. The Calculation of Magnetic Fluxes and Eddy Currents in Generator Stator Cores. Proc. 1st COMPUMAG Conf., Oxford, April 1976, Section 7, p. 255.
2. Phemister, T.G. and Wymer, C. The Effect of Gaps between Laminations in an Idealised Stator Core. Proc. 2nd. COMPUMAG Conf., Grenoble, Sept. 1978.